TARGETING THE NITRIC OXIDE SIGNAL TRANSDUCTION PATHWAY AS A POTENTIAL OCULAR HYPOTENSIVE

By

WILLIAM MICHAEL DISMUKE

A DISSERTATION PRESENTED TO THE GRADUATE SCHOOL
OF THE UNIVERSITY OF FLORIDA IN PARTIAL FULFILLMENT
OF THE REQUIREMENTS FOR THE DEGREE OF
DOCTOR OF PHILOSOPHY

UNIVERSITY OF FLORIDA

2009

To my parents, Bill and Nancy

ACKNOWLEDGMENTS

I thank my parents.

TABLE OF CONTENTS

page

LIST OF FIGURES

Abstract of Dissertation Presented to the Graduate School
of the University of Florida in Partial Fulfillment of the
Requirements for the Degree of Doctor of Philosophy

TARGETING THE NITRIC OXIDE SIGNAL TRANSDUCTION PATHWAY AS A POTENTIAL OCULAR HYPOTENSIVE

By

William Michael Dismuke

December 2009

Chair: Dorette Z. Ellis
Major: Pharmaceutical Sciences - Pharmacodynamics

Nitric oxide donors decrease intraocular pressure by increasing aqueous outflow facility in the trabecular meshwork and/or Schlemm's canal however the cellular mechanisms are unknown. Cellular mechanisms known to regulate outflow facility include changes in cell volume and cellular contractility. In this study we investigated the effects of nitric oxide donors on outflow facility. Additionally, we examined the nitric oxide -induced effects on trabecular meshwork cell volume, the signal transduction pathway(s) and ion channel involved. A novel protocol was used to measure cell volume in individual primary human and porcine trabecular meshwork cells. Cell volume was measured using Calcein AM fluorescent dye, detected by confocal microscopy and quantified using NIH ImageJ software. Inhibitors and activators were used to characterize the involvement of nitric oxide, soluble guanylate cyclase, cyclic GMP, protein kinase G and BK_{Ca} channel. An anterior segment organ perfusion system measured outflow facility. Exposure of trabecular meshwork cells to nitric oxide resulted in decreased cell volume and these decreases were abolished by ODQ and the BK_{Ca} channel inhibitor, IBTX, suggesting the involvement of soluble guanylate cyclase and K^+ eflux respectively. The nitric oxide -induced decreases in cell volume were mimicked by 8-Br-cGMP and abolished by the protein kinase G inhibitor, (RP)-8-Br-PET-cGMP-S suggesting the involvement cGMP and

protein kinase G pathway. Additionally, the time course for the nitric oxide -induced decreases in trabecular meshwork cell volume correlated with nitric oxide -induced increases in outflow facility suggesting that the nitric oxide -induced alterations in cell volume may influence outflow facility.

CHAPTER 1
INTRODUCTION

Intraocular Pressure and Glaucoma

Elevated intraocular pressure (IOP) puts a patient at an increased risk for developing visual field loss, in the progressive blinding disease, glaucoma. IOP results from the balance between aqueous humor secretion by the ciliary processes and outflow through the trabecular meshwork and Schlemm's canal. The major route for the outflow of aqueous humor is the trabecular meshwork [1] [2] comprising of uveal and corneoscleral trabecular meshwork [1] and the juxtacanalicular cells (JCT-trabecular meshwork) [3], in conjunction with the Schlemm's canal. An improper balance of aqueous humor secretion and outflow will yield high pressures within the eye. Through an unknown mechanism, this elevated IOP increases the likely hood of retinal ganglion cell death. As retinal ganglion cells are lost, the patients vision is progressively lost as well, both of which are irreversible. Since we are currently unable to repair the damage from the loss of the retinal ganglion cells, the only viable therapy for patients with ocular hypertension is management of IOP.

Currently IOP can be managed by two major methods, ocular hypotensive drugs or surgery. The surgical methods to reduce IOP are numerous and well outside the scope of these studies. In general they are intended to increase the drainage of aqueous humor from the eye, but from here on will not be mentioned. Our focus will be on pharmacological methods to reduce IOP. To lower IOP, ocular hypotensive drugs generally work by reducing the production of aqueous humor or increasing the drainage of aqueous humor. Inhibitors of carbonic anhydrase, an enzyme involved in aqueous humor secretion, lower IOP by reducing aqueous humor production. Conversely, prostaglandin analogs lower IOP by increasing the drainage of aqueous humor from the eye. While both of these IOP lowering strategies are effective, these studies will

focus on the outflow of aqueous humor, as dysfunctions in aqueous humor outflow are thought to underlie the IOP increases in the most common form of glaucoma, primary open angle.

Cellular Mechanisms that Regulate Outflow Facility

Once thought to be a passive process, the outflow of aqueous humor is now known to be actively controlled by the cells in the aqueous humor outflow pathway. Several mechanisms have been characterized by which changes in aqueous humor outflow can occur. These include trabecular meshwork contractility and cell volume changes, ciliary muscle contractility, alterations of the ECM in the trabecular meshwork and pore formation and vacuoles in the inner wall of the Schlemm's canal[4-10] . This research focuses on trabecular meshwork cell volume changes and the role it plays in regulating outflow facility. Our goal is to identify a signal transduction pathway in trabecular meshwork cells by which nitric oxide and NO- independent sGC activators mediate increases in aqueous humor outflow.

Cell volume changes in the aqueous humor outflow pathway are of interests to study as they have been correlated with changes in outflow facility. Previous studies demonstrate that a hypotonic or hypertonic challenge to a perfused eye anterior segment will decrease or increase outflow facility respectively[7] . To begin to hypothesize a mechanism by which changes in trabecular meshwork cell volume would affect aqueous humor drainage we must understand the architecture of the aqueous humor outflow pathway. The trabecular meshwork is composed of interwoven collagen covered elastin "beams". Trabecular endothelial cells (trabecular meshwork cells) line the outflow pathway and have been suggested to perform a number of functions including phagocytosis[11] and extracellular matrix turnover[12] . As aqueous humor flows deeper into the trabecular meshwork, toward the Schlemm's canal, the open spaces available for fluid to flow through decrease. As the space for fluid flow decreases, the volume of the trabecular meshwork cells lining these openings would begin to exert more influence over outflow facility.

Increasing or decreasing the volume of these cells would therefore decrease or increase the rate by which fluid flows exits the eye, respectively. To understand the components involved in maintaining and/or returning to resting cell volume and basal outflow facility, investigators have utilized perfused eye anterior segments.

Using this technique, several ion channels have been implicated in mediating the recovery to baseline outflow facility following a hypotonic or hypertonic challenge. Recovery from a hypotonic challenge was slowed and the magnitude of the decrease in outflow facility was greater in the presence of the BKca channel inhibitor iberiotoxin. The opposite effect was seen when the BKca channel activator NS1619 was included with the hypotonic challenge. Recovery to baseline outflow quickened and the magnitude of the outflow facility reduction was decreased. This study also implicated the chloride swell channel in mediating a recovery for hypotonic challenge as the channel blocker tamoxifen produced effects similar to iberiotoxin[5] . Additionally, the Na, K, 2Cl co-transporter blocker bumetanide, which has been shown to decrease TM cells volume[6] , increased outflow facility in an eye anterior segment perfused with isotonic medium[7] . While these mechanisms have been experimentally shown to contribute to the regulation of aqueous humor outflow, the possibility exist that other unknown mechanisms also contribute.

Nitric Oxide Regulation of Intraocular Pressure

The gaseous signaling molecule nitric oxide (NO) has been shown to regulate both the production and outflow of aqueous humor. NO mediates many of its effects through soluble guanylate cyclase (sGC) and increases in cyclic GMP (cGMP). Because the binding of NO to sGC results in decreased IOP, the study of the activation sGC in the tissues of the aqueous humor outflow pathway, becomes critically important since it may provide new targets for the development of ocular hypotensive drugs.

NO is a diatomic gas with a very short half-life of just a few seconds [13] . It is produced by a family of enzymes, the nitric oxide syntheses (NOS), through the conversion of L-Arginine to NO and L-citrulline. The active enzyme is composed of a heme-bound homodimer assembled from heme-deficient monomers. There are 3 major types of NOS in mammalian tissue; endothelial NOS (eNOS), neuronal NOS (nNOS) and inducible NOS (iNOS). eNOS and nNOS are expressed constitutively, and are capable of producing low levels of NO, <1uM [14] . NO production it thought to have two distinct roles in the body; production of an autocrine/paracrine signaling molecule and production of a toxic free-radical gas. With all three isoforms producing the same molecule, the pathophysiological implications of any inappropriate NO production must be kept under consideration.

NO generated by nNOS and eNOS has been shown to activate cyclic-nucleotide-gated channels, protein kinases, and phosphodiesterases [15] . These physiological processes may be considered 'low concentration' effects, requiring less than 1 micromolar of NO [14] . High concentrations of NO produced by iNOS can result in auto-oxidation and the production of dinitrogen trioxide [16] , which is the primary mechanism of nitrosylation in which nitrosothiols of cysteines are formed. In addition, strong oxidants such as superoxide (a reactive oxygen species) can act with NO to form peroxynitrite [17] which reacts with the phenol moiety of tyrosine resulting in nitration of tyrosine residues in proteins. Both nitrosylation and nitration of tyrosine residues have been shown to affect protein function. The implications of these findings on the effect of high concentrations of NO to increase aqueous humor outflow and NOs effect on retinal ganglion cells are unknown. This is outside the scope of our study, but must always remain under consideration. Here we will focus on the effects of low, physiologically relevant concentrations on NO such as produced by nNOS or eNOS.

NO mediates its physiological effects by binding to sGC. Once bound to sGC, it causes the conversion of GTP to 3'-5'-cyclic guanosine monophosphate (cGMP). cGMP will then go on to interact with various cyclic-nucleotide gated channels, protein kinases and protein phosphodiesterases to produce physiological effects.

Other Activators of Soluble Guanylate Cyclase

In addition to the endogenous sGC activator NO, compounds such as YC-1 have been shown to activate sGC independent of NO[18] and decrease IOP[19] . Though the mechanism by which YC-1 activates sGC is not fully understood, it thought to affect the positioning of the heme in the enzyme[20] or enhance the activation of sGC by NO[21] . With evidence of a decreased ability to produce NO in the trabecular meshwork of glaucomatous eyes[22] , it is also of interest to note the reported synergistic effect of YC-1 on the NO-induced stimulation of sGC[23] . This suggests the possibility that drugs like YC-1 may be used, not only to activate sGC, but also to amplify the diminished, endogenous NO production capacity suggested by the above mentioned study. In addition to YC-1-like, heme-dependent sGC activators, several heme-independent sGC activators have been characterized. These compounds, like BAY-58-2667, are reported to activate sGC even though the heme may be absent or oxidized[24] , a state in which NO cannot activate sGC. With the complexities of NO's participation in the redox state of a cell, as well as the ability of YC-1 to act synergistically with NO and BAY-58-2667 to activate sGC independent of heme, it is of significant clinical interest to investigate the ability of NO-independent sGC activators to affect outflow facility and volume changes in trabecular meshwork cells.

Direct Activation of the Large-conductance, Calcium-activated Potassium Channel

With the above mentioned studies on the influence of the BKca channel on recovery of basal outflow facility following a hypo- or hypertonic challenge, studies demonstrating the

cGMP-induced activation of this channel in bovine trabecular meshwork cells [25] and studies demonstrating the channels involvement in cGMP-induced relaxation of isolated bovine trabecular meshwork strips[26] , we are interested in investigating the role BKca channel activation plays in regulating trabecular meshwork cell volume and outflow facility.

The BKca channel is a potassium channel, with its activity regulated endogenously by membrane potential, intracellular calcium concentration[27] and cGMP-dependent protein phosphorylation events[28, 29] . By allowing a large efflux of potassium, when opened, the channel is capable of hyperpolarizing the cell. That and the ability of cGMP- dependent protein phosphorylation to modulate channel activity led investigators to test and demonstrate the involvement of the BKca channel in the NO-induced relaxation of smooth muscles. With this in mind, we examine the role the BKca channel plays in the NO\cGMP-induced increases in outflow and decreases in trabecular meshwork cell volume, as well as the role the channel plays in restoring resting cell volume following a hypo- or hypertonic challenge. To do this we utilize a well characterized, BKca channel blocker iberiotoxin (IBTX)[30] . In addition to the endogenous BKca activity modulators mentioned above, several compounds have been synthesized that are reported to directly activate the channel. For our studies we will use the benzimidazolone derivative, NS1619 as our BKca channel activator[31] .

CHAPTER 2
MATERIALS AND METHODS

Cell Culture

For our in vitro studies we obtained human donor eyes with no history of ocular disease or surgery from Lions Eye Institute (Tampa, Fl) within 24-30 hours postmortem. Primary human TM cell lines were developed and named according to the age of the donor (ie HTM80). Prior to dissection, eyes were stored in a moist environment at 4°C. Porcine eyes were procured from the local abattoir within 1 hour postmortem, stored in PBS and kept on ice. To kill any containments on the exterior of the eye, the eye is submerged in a 1:1 solution of phosphate buffered saline solution (PBS) and Betadine (providone-iodine, 7.5%) for 3 minutes, then rinsed three times in PBS. Following that, standard ophthalmic microsurgery instruments were used to hemi-sect the eye and remove the lens, iris and ciliary body. The remaining anterior portion of the eye is bisected and the TM was removed from both halves using forcepts. The TM stripes were them placed in a filtered solution containing 5mL PBS, 5mg collagenase type IV and 75uL human albumin. This solution containing TM explants was vigorously shaken and placed in a 37°C water bath for 30 minutes, with additional vigorous shaking at 10 minute intervals. This process is intended to breakdown the type 4 collagen, an ECM component upon which trabecular meshwork cells are thought to directly attach[32] , thus increasing the likelihood trabecular meshwork cells will migrate off the dissected TM strips and onto culture dishes. However, long term exposure to the collagenase solution may have negative effects on the proliferation of the cells in the culture dish and needs to be removed. To remove the collagenase, the tube containing TM explants and collagenase solution was centrifuged at 800 x g for 8 minutes. The resulting supernatant was aspirated and the pellet resuspended in 5mL of low glucose (1 g/L) DMEM (Mediatech, Herdon, VA) containing 10% (v/v) FBS, 100 U/mL penicillin and 100 ug/mL

streptomycin and transferred to one well of a gelatin coated 6-well plate. Cells were grown in a tissue culture incubator at 37°C in 5% CO2. Confluent cells were trypsinized and passaged.

To ensure the human cells we have cultured are indeed from the trabecular meshwork they were validated by their morphology and the presence of dexamethasone-induced myocilin expression. Specifically trabecular meshwork cells *in vivo* produce a mutant form of the protein myocilin when exposed to synthetic glucocorticoids such as dexamethasone. This is the etiology underlying the steroid-induced form of glaucoma. To use the trabecular meshwork cells sensitivity to dexamethasone to validate their origin, we use immunocytochemistry and a polyclonal myocilin antibody[33] . We grew the suspected TM cells on chambered slides to 80% confluency. Dexamethasone (100nM) in DMEM with 10% fetal bovine serum was added to the cells. The cells were exposed to dexamethasone for 7 days, washed in PBS, fixed in ice-cold methanol for 7 minutes, washed in PBS again and stored at -20°C. The slides were thawed on the benchtop, washed with TBST and blocked in 5% goat serum for 1 hour. The polyclonal myocilin antibody in TBST (1:1000) was added to the slide and incubated at 4°C in a moist environment overnight. The slides were washed three times in TBST and a Cy3-conjugated goat anti-mouse secondary antibody in TBST (1:1000) was incubated for two hours at room temperature.

Porcine TM cells were validated by their ability to take up acetylated LDL labeled with BODIPY FL and secrete tissue plasminogen activator.

Human and porcine TM cells were serum-starved for 48 hours prior to being used in experimental protocols. For our experiments, cells from passage 3-5 were used.

Outflow Facility Measurements

Porcine eyes were obtained from a local abattoir within 1 hours of the animal's death and kept in DPBS on ice prior to dissection. Standard ophthalmic microsurgery instruments were used to hemi-sect the eye and remove the lens, iris and ciliary body. The dissected anterior

portion of the eye was mounted in an anterior segment organ culture perfusion chamber. The anterior segment is then placed in a cell culture incubator kept at 37°C in 100% humidity with a 5% CO_2 atmosphere and perfused at a constant 14mmHg. The perfusate for these studies was low glucose (1g/L) DMEM with 100 U/ml penicillin and 100 μg/ml streptomycin. Outflow facility is calculated as the loss of perfusion media from the supply bottle, determined by weight, over time divided by the constant pressure of 14mmHg. The anterior segments were allowed to perfuse for 12 to 48 hours prior to drug treatments to allow for the establishment of a stable basal outflow facility. To administer experimental treatments to the anterior segment, a constant pressure fluid exchange system was used. This system allows for the complete exchange of the media contained in the artificial anterior chamber (~600μL) without a change in pressure, giving us the ability to apply a bolus of the experimental treatment. Outflow facility measurements are recorded by a computer every minute for the entire duration of the anterior segments perfusion. For the analysis, each perfusion experiment is normalized to its mean baseline outflow facility, giving us a ratio of the pre- and post-treatment outflow facilities (C_0/C_D) facility [7, 34, 35] . The data from several perfusion experiments are pooled and an ANOVA and Holm-Sidak post-hoc tests are performed to determine any statistically significant effect of the experimental treatment on outflow facility.

Cell Volume Measurements

Previous studies examining changes in trabecular meshwork cell volume could not measure the volume of a single trabecular meshwork cell over time that was firmly attached to its substrate[6, 36] , the normal state for a trabecular meshwork cell *in vitro*. To achieve this, we utilized cultured human and porcine trabecular meshwork cells and a laser scanning confocal microscope. Low passage human and porcine TM cells (passage 2-5) in either collagen-coated

Lab-Tek II chambered coverglass (Nalge Nunc) or collagen-coated 35mm FluoroDishes (WPI Inc) were grown to confluency. These cells were then serum-starved for 48 hours prior to the start of the cell volume measurements. The TM cells were incubated with the fluorescent dye Calcein AM (Molecular Probes) at a concentration of 1μM for 1 hour in a tissue culture incubator at 37°C in 5% CO2. The original, membrane permeable, nonfluorescent acetylmethyl ester (AM) form of the dye diffuses into the cells where it undergoes acetylmethyl ester hydrolysis, becoming membrane impermeable and fluorescent. We use this intracellular fluorescence as a marker for intracellular volume.

Low passage TM cells incubated with calcein were removed from the tissue culture incubator and placed on the microscope stage. Cells were visualized with a 20X objective and a region of cells was selected for the capturing of confocal image stacks. Individual confocal images were captured in an 8-bit, 1024x1024 or 512x512 pixel format. Spacing between images in the image stack was set at 1μm. To ensure that both the upper and lower portions of the cells being imaged were included in the image stack, we were mindful to set the upper and lower bounds of the area to be scanned, at least 1μm above and below where the cells upper and lower portion appeared to be. To capture images of the same cells over time, we set the microscope to capture image stacks at 5 minute intervals for 20 minutes. The first image stack is captured and upon completion, our experimental compound is carefully pipetted into the dish containing our cells. The microscope will capture four additional image stacks 5, 10, 15 and 20 minutes following the addition of our experimental compound. For studies involving enzyme or ion channel inhibitors, the inhibitor was added 5 minutes prior to capturing the initial image stack. However, for experiments involving a hypo- or hypertonic challenge a modification of the above protocol was needed as five minute intervals for volume measurements were too long to capture

the rapid volume changes induced by tonicity changes. The need to quickly capture image stacks for each time point required we reduced our resolution to 512x512 and increased the scan speed from 400hz to 700hz. This increase in scan necessitates a 1.7 ratio digital zoom, reducing the number of cells per treatment we could image. By altering our protocol this way, we can capture a complete z-stack with a 1μm z-spacing in less than 1 minute, allowing us to take an initial, resting cell volume measurement, add our hypo- or hypertonic solution then scan the cells at a 1 minute interval for 10 minutes.

To quantify cell volume measurements from the confocal image stacks we utilize NIH ImageJ software and a custom voxel counting macro. First we must determine a fluorescence intensity threshold value to allow us to mark the boundary between intracellular and extracellular space. To do this we image fluorescent microspheres of known diameter and volume that have similar fluorescence intensity as our calcein incubated cells. Our confocal images were captured with an intensity resolution of 8-bits or 256 (ie 2^8) shades from light to dark. In defining a threshold value to use in our cell volume analysis, we selected a brightness between 0 and 255, which will thereafter define the intracellular (bright from calcein fluorescence) and extracellular (dark) space. To select this threshold value, we analyze the volume of a number of the fluorescent microspheres using all 256 possible threshold values. The threshold value yielding the most accurate microsphere volume (known from the manufacture) will then be used as the threshold value for further cell volume analysis. Image stacks from the experiment are then imported into ImageJ and the outer, lateral boundary of each cell in the first image stack (the initial or “0” time point, without drug) is defined by hand (known as a “region of interest” or ROI) and saved. The threshold value determined above is then applied to the image stack, yielding a black and white or binary image and all thresholded pixels (black) within each ROI

are counted for each image in the image stack. The resulting number is the voxel count, a number representing the volume of each cell in the image stack. This number is used as the initial, resting cell volume, prior to drug treatment. Similarly, we imported the image stack from the next time point and ran the voxel counting macro again, using the saved RIO's from the initial (0 time point) image stack. By ensuring that the microscope stage did not shift during our experiment the RIOs defined in the 0 time point image stack should also accurately define the outer boundary of each cell in the subsequent image stacks. The voxel counts for each cell, at each time point was then imported to a spreadsheet. To represent this data as a percentage change in cell volume, we divide the voxel count for each cell at each time point by the voxel count of that cell at the 0 time point. Statistical comparisons were performed by ANOVA followed by the Holm-Sidak or Fisher least significant difference method for the comparison among different means.

Drug Preparation

- DETA-NO (1-[N-(2-Aminoethyl)-N-(2-ammonioethyl)amino]diazen-1-ium-1,2-diolate)
    - Solid dissolved in deionized water, 296mM stock
- ODQ (1H-[1,2,4]oxadiazolo[4,3-a]quinoxalin-1-one)
    - Solid dissolved in DMSO, 27mM stock
- Rp-8-Br-PET-cGMPS
    - Solid dissolved in deionized water, 4.36mM stock
- IBTX (Iberiotoxin)
    - Solid dissolved in deionized water, 10μM stock
- Hypertonic solution
    - D-mannitol dissolved in DMEM, 300mM stock
- Hypotonic solution
    - DMEM:deionized water (2:3, v:v)
- YC-1(3-(5'-hydroxymethyl-2'-furyl)-1-benzylindazole)
    - Solid dissolved in DMSO:Ethanol (1:1), 30mM stock

    - Working solution, 30mM stock:DMEM:DMSO:Ethanol (2:2:1:1)
    - Working solution kept at 37°C until use
    - Use immediately

- BAY-58-2667
    - Solid dissolved in DMSO:Ethanol (1:1), 30mM stock
    - Working solution, 30mM stock:DMEM:DMSO:Ethanol (2:2:1:1)
    - Working solution kept at 37°C until use
    - Use immediately

- NS1619 (1,3-Dihydro-1-[2-hydroxy-5-(trifluoromethyl)phenyl]-5-(trifluoromethyl)-2H-benzimidazol-2-one)
    - Solid dissolved in Ethanol, 13.8mM stock

CHAPTER 3
NO-INDUCED REGULATION OF HUMAN TRABECULAR MESHWORK CELL VOLUME AND AQUEOUS HUMOR OUTFLOW FACILITY INVOLVE THE BK_{CA} ION CHANNEL

Introduction

Maintenance of correct intraocular pressure (IOP) is a requirement for good vision. Two major factors contribute to IOP, production of aqueous humor by the ciliary processes and the outflow of aqueous humor through the trabecular meshwork (TM) and Schlemm's canal; thus increases in production and/or decreased in outflow facility of aqueous humor could result in high IOP. In fact, increased resistance to aqueous humor outflow through the juxtacanalicular region of the TM has been implicated in primary open angle glaucoma [37] , a blinding disease that affects millions of people worldwide. Decreasing IOP is a viable strategy for preventing blindness caused by glaucoma and slowing its progression.

The TM is comprised of three anatomical regions, the uveal, corneoscleral and the juxtacanalicular regions [3, 38] ; with two distinct cell populations [39] . The cellular mechanisms underlying changes in aqueous humor outflow througth the TM are not well understood: however, several cellular mechanisms have been proposed [40] . The TM is thought to be a smooth muscle-like tissue with contractile properties [41, 42] . Contraction and relaxation of the cells are thought to regulate aqueous humor outflow [43-46] . Similarly, increases or decreases in the volume of TM cells could influence outflow. [5-7, 47-49] . Trabecular meshwork cell volume is influenced by the activities of the Na-K-2Cl exchanger [4, 6, 7] the Na+/H+ transporter [36] , and the K+ and Cl- channels [5, 36] .

Further, it is possible that both the cellular contractile mechanisms and the cell volume regulatory mechanisms are functionally linked [50-52] as the large conductance calcium-activated potassium channel (BK_{Ca}), have been shown to regulate TM cell volume and contractility [5, 45] and outflow facility [5] .

The BK_{Ca} channels are activated by increased calcium [53, 54], changes in cell membrane voltage [55] or neurotransmitters including NO [28, 56]. In cerebral artery smooth muscle cells the phosphorylation of the α subunit of the BK_{Ca} channel by PKG has been shown to mediate the NO-induced activation the BK_{Ca} channel [28].

The human TM is enriched with the NO producing enzyme, nitric oxide synthase (NOS), particularly endothelial NOS (NOS-III) [57] and nitrinergic nerve terminals [58]. NO donors reduced IOP in both normal [59] and glaucomatous rabbit eyes [60] without systemic effects [59]. Additionally, intracameral injection of NO donors decreased IOP by increasing outflow of aqueous humor [61]. Similarly intravitreal and intracameral injections of NO donors in rabbits caused drastic decreases in IOP, concurrent with nitrite production the measurable result of NO production [62]. Other studies have shown that NO donors reduce IOP in monkeys through an action on outflow resistance [35]. While NO donors effectively reduce IOP, the signaling cascade mediating the cellular response in this tissue is unknown. The present study was designed to elucidate the mechanism of response of the TM to NO

We tested the hypothesis that NO donors regulate TM cell function by decreasing TM cell volume. We tested the involvement of a regulatory pathway by which NO acting via activation of sGC, cGMP, and PKG decrease TM cell volume. We also examined the role of BK_{Ca} channel in the NO-induced decreases in cell volume and the NO-induced increases in outflow facility and determined if the time course for the NO-induced decreases in TM cell volume correlated with the NO-induced increases in outflow facility.

Materials and Methods

Tissue

Because morphological and biochemical studies suggested that the porcine anterior chamber perfusion model can be correlated with the human perfusion system [63], perfusion studies were performed using porcine eyes. Cellular studies were performed in human primary TM cells and parallel studies were performed in primary porcine TM cells.

Cell Culture

Eyes from human donors with no history of ocular disease or surgery were obtained from Lions Eye Institute (Tampa, FL) within 24-30 hours postmortem. Primary human TM cell lines (numbers representing ages of the donors) (HTM44; generous gift of Dr. D. Stamer, HTM26, HTM71, HTM36, HTM80 and HTM86) were developed. For our experimental protocols cells from early passages (3-5) were used. Human TM explants were obtained either from whole eyes that were stored in a moist environment at 4^{o}C or from corneal scleral rims stored in Optisol (Dexol; Chiron Ophthalmics, Irvine, CA) at 4^{o}C. Porcine eyes were obtained from the local abattoir within 1 hour postmortem and maintained on ice. We used standard ophthalmic microsurgery instruments to bisect the eyes and remove the cornea, iris, lens and ciliary body. TM cells were isolated after collagenase digestion of TM explants [64]. Collagenase-treated cells were grown in low glucose (1g/L) DMEM (Mediatech, Herdon VA.) in the presence of 10% fetal bovine serum (Mediatech, Herdon VA.), 100 U/ml penicillin and 100 μg/ml streptomycin (Mediatech, Herdon VA.). Cells were grown in 6-well culture dishes (Nalge Nunc International, Rochester, NY) in a tissue culture incubator @ 37^{o}C in 5% CO_2. Confluent cells were trypsinized and passaged. We validated human TM cells by their morphology and the presence of dexamethasone-induced myocillin expression [33]. To identify porcine TM cells we used the ability of TM cells to take up acetylated low-density lipoprotein and secrete tissue plasminogen

activator. For experimental protocols, TM cells were grown on Lab-Tek ll chambered cover glass (Nalge Nunc International, Rochester, NY) in low-glucose DMEM as described above to 100% confluency, after which they were exposed to serum free media for 2 days prior to performing the experiments.

Measurement of Cell Volume

Cell volume measurements were performed using the modified protocols of Mitchell et al and Bush et al [36, 65, 66] . Prior to any drug treatments, the cells were loaded with the fluorescent dye Calcein AM in DMEM at 37°C, in 5% CO_2 incubator for 60 minutes to ensure a stable baseline. The coverslips containing the cells were subjected to confocal microscopy using a Leica confocal microscope. For some experiments a Leica confocal microscope with a platform containing a 37°C, 5% CO_2 incubator was used.

We developed a technique of drug delivery to the TM cells on the cover slips to ensure that the slides did not shift during imaging and that images would be taken of the same cells. Specifically, several ports were drilled in the covers of the glass chambers. Tubes attached to syringes were inserted into each port allowing for the exchange of media and drugs. Images were taken without drug treatment, (0) time point, this served as the experimental control. Drugs were then added to the cells through the ports without shifting the cover slip. Images were taken of the same cell (s) at varying time periods following application of the drugs. Additionally, images were taken of cells that were not exposed to drugs at the time periods indicated above to serve as controls for evaluating the stability of the dye. In some experiments media containing drugs were carefully removed from the cover slip and fresh media was added. Images were taken of the same cells and changes in cell volume were quantified. To assess the functioning of the volume regulatory mechanisms in TM cells the osmolarity of the media was changed. Hypertonic medium was made by addition of 150 mM mannitol to DMEM (~469 mOsm/kg) and

hypotonic medium was made by addition of deionized water to DMEM for a final concentration of 30% water and 70% DMEM (~208 mOsm/kg).

For our experiments, the microscope captured either a 1024 x 1024 or a 512 x 512 pixel image with 8-bits of resolution (256 colors). The confocal microscope captures images in three dimentions, allowing the NIH ImageJ software to identify the top and bottom edges of the cell. Images were converted from 8-bit to binary values using a threshold that was determined by analysis of fluorescent Fluoresbrite latex beads (Polyscience Inc., Warrington) of known diameter and volume that were imaged under conditions identical to those used for TM cells. A region of interest was then selected around each cell and the ImageJ software was used to calculate the number of voxels in the region of interest in the image stack. Changes in cell volume were determined by dividing the voxel count with drug treatment by the voxel count without drug treatment.

Outflow Facility Measurements

Anterior segment perfusion organ culture was used to measure outflow as described by Johnson et al [67, 68]. Porcine eyes were obtained from the local abattoir and maintained on ice following enucleation and bisected within 2 hours postmortem. Eyes were bisected at the equator and the iris, lens and ciliary processes were removed. The anterior segments were cultured at 37°C in 100% humidity at 5% CO_2 atmosphere and perfused at constant pressure of 14 mmHg [69, 70]. The outflow rates were determined gravimetrically as the changes in weight of the medium as the eyes were perfused over time. The data were captured at one minute intervals by WinWedge software attached to the balance and recorded in an Excel spread sheet; outflow facility was expressed as μl/min/mmHg perfusion pressure. Organ perfusions were performed with isotonic DMEM (~309 mOsm/kg) to establish baseline facility followed by perfusion with

several experimental conditions: hypotonic, and hypertonic media (to establish that the volume regulatory mechanisms are functional) and the NO-donor, diethylenetriamine nitric oxide (DETA-NO) (100μM). Hypotonic and hypertonic media were made as described above. After a stable baseline was established, the drugs were delivered via a drug exchange system which supplied a bolus of drug. Specifically, a 10 ml syringe, held at a height above the mounted anterior segment and containing DMEM + drugs was attached to one of the perfusion chamber's ports. Another 20 ml waste syringe, held below the mounted anterior segment, was attached to a chamber port and this line was clamped. By slightly opening the clamp to the waste syringe, the anterior chamber medium was slowly exchanged with the medium in the drug supply syringe in a manner that prevented any changes in the perfusion pressure. After medium containing drugs was in the chamber, entry to this port was clamped and flow of medium without drugs was restarted through a third port.

The viability of the tissue was evaluated using live-dead stain (Molecular Probes, Carlsbad, CA), which stained for the total number of nuclei in the TM, following perfusion. Specifically, flatmount intact TM tissue was treated with live-dead stain and visualized using confocal microscopy. Live cells were stained with the green fluorescence and dead cells were stained with red fluorescence. Cellular viability was determined to be good and data usable when 85-90% of the total cells stained with green fluorescence [9] .

Materials and Reagents

Routine reagents and iberiotoxin (IBTX) were purchased from Sigma (St. Louis, MO). Others were obtained as follows: 8-bromo-cGMP sodium salt, 1*H*-[1,2,4]oxadiazolo[4,3-a]quinoxalin-1-one (ODQ), and diethylenetriamine NO (DETA-NO) from Sigma-RBI (Natick, MA); (RP)-8-Br-PET-cGMP-S from Calbiochem (La Jolla, CA).

Statistics

Statistical anylasis was performed using ANOVA, followed by Holm-Sidak method for comparison of significant difference among different means.

Results

NO Donors Increase Outflow Facility

Outflow facility was measured in porcine anterior eye segments as described. Freshly dissected eye anterior segments were allowed to adapt to their new environment during which time outflow facility increased for the first 3 – 8 hours a phenomenon referred to as "wash-out" [70, 71] after which outflow facility remained stable [63]. Basal outflow facility (pre-drug treatment) was 0.2373-0.5220 μl/min/mmHg among experiments and was stable for several hours prior to drug treatment and remained stable post drug effect. Because of the stability of the outflow facility baseline after the initial "wash-out" period, it was not necessary to correct for non-drug related changes in outflow facility in our experimental protocol.

After a stable baseline was established DETA-NO (100μM) was added to the perfusate and resulted in a significant increase in outflow facility Figure 3-1A. Outflow facility was increased at 10 minutes and reached its maximal level at 20 minutes following application of the DETA-NO. The maximal effect of the drug was sustained for 1.5 hours after which outflow facility returned to values similar to baseline outflow facility between 5-6 hours post drug application. We observed significant increase in outflow facility (0.4884 - 1.3956 μl/min/mmHg; mean 0.8635 μl/min/mmHg + SEM 0.1029) over baseline values in response to DETA-NO in 8 separate experiments.

We tested the ability of the outflow pathway to respond to changes in osmolarity preceding NO treatment. This allowed us to determine that the perfused eye segments were healthy and

responded with expected changes in outflow facility when challenged with changes in osmolarity. Figure 3-1B demonstrates that exposure of porcine eye anterior segments to perfusion with hypertonic media resulted in a significant increase in outflow facility (40% above baseline) after which outflow facility returned to baseline. The eyes were perfused for 19 hours with DMEM only and the baseline values decreased slightly but remained constant for several hours. Subsequently a bolus of DETA-NO was added to the porcine anterior segment and allowed to perfuse. Figure 3-1B demonstrates that as with figure 3-1A, DETA-NO increased outflow facility after the eye had previously responded to hyperosmotic challenge.

NO donors are known to activate the BK_{Ca} channels resulting in the efflux of K^+ from the cell. We wished to determine the involvement of BK_{Ca} channels in the NO-induced regulation of outflow facility. After baseline outflow facility was determined, anterior segments were perfused with DETA-NO as described. IBTX (50 nM) [5, 25] was added to the perfusate after the NO-induced increase in outflow facility was observed. Addition of IBTX resulted in a significant decrease in the NO-induced response in outflow facility within 10 minutes after the IBTX was added (Figure 3-1C).

NO Decreases TM Cell Volume

Agents known to decrease TM cell volume also increase outflow facility. Others have demonstrated that NO decreases ventricular cell volume [72]. Therefore, we wanted to determine if changes in cell volume are cellular mechanisms by which NO modulated TM cell function. To quantitatively measure changes in cell volume, HTM cells (HTM26, HTM44 and HTM86) were incubated in Calcein AM dye and subsequently exposed to the NO donor, DETA-NO. Z-stack images demonstrate that DETA-NO (100μM) decreases TM cell volume (Figure 3-2A). To determine the concentration needed to decrease cell volume, early passage human TM cells were

exposed to varying concentrations of DETA-NO (1 - 300 μM). Images were taken without drug treatment (0) time point which served as a control for the treatment groups. Drugs were then added to the cells and images were taken of the same cells at 20 minutes. Figure 3-2B demonstrates that DETA-NO elicited a dose-dependent decrease in human TM cell volume with maximal effects procduced by 100 and 300 μM.

We also tested the reversibility of the DETA-NO- induced decreases in TM cell volume. . In our hands Calcein AM is stable for up to 1 hour post Calcein AM incorporation into cells and exposure to laser treatments. Therefore all experimental treatments needed to be done within 1 hour time period. Because in our preliminary studies we had observed significant decreases in TM cell volume at 10, 15 and 20 minutes of exposure to DETA-NO, TM cell were for 10 minutes. TM cells were incubated with Calcein AM as previously described and images were captured without drugs. Subsequently, the cells were treated with DETA-NO (100 μM), and images were captured at 10 minutes post-drug treatment. The medium containing drug was removed and replaced with fresh medium and the cells were then incubated for 30 minutes in DMEM only at 37°C in 5% CO_2 and images were captured. Figure 3-2C demonstrates that cells exposed to DETA-NO resulted in significant decreases in cell volume which were reversed following removal of the drug.

Changes in Cell Volume in Response to Changes in Osmolarity

To assess the function of volume regulatory mechanisms in TM cells we exposed both early passage human (HTM80, 86) and porcine TM cells to hypo- and hypertonic DMEM which would be expected to cause swelling and shrinkage of the cells respectively. TM cells were incubated with Calcein AM as described and stable baselines were established. Images were captured at 0 time point in isotonic medium (control) after which the osmolarity of the medium

was altered. Porcine TM cell volume was altered in response to hypotonic as well as hypertonic medium (Figure 3-3A). There was a 12.4 % increase in TM cell volume after the medium was changed from isotonic to hypotonic. Thereafter, TM cell volume gradually decreased without changes in osmolarity of the medium. Exposure of TM cells to hypertonic medium resulted in 16.2 % decrease in cell volume post isotonic changes and cell volume increased after hypertonic medium was exchanged with isotonic medium at 37^{o}C in 5% CO_2 (Figure 3-3A).

Figure 3-3B demonstrates that exposure of human TM cells to hypotonic medium resulted in 11 % increase in cell volume. Images were captured of cells treated with isotonic medium, after which cell were exposed to hypotonic medium and images were captured within 1 minute of exposure of cells to anisosmotic medium. There was an increase in TM cell volume which peaked within 3 minute after the medium was changed from isotonic to hypotonic and returned to baseline. We then tested the involvement of the BK_{Ca} channel in the TM volume regulatory mechanism. Calcein AM loaded cells were exposed to hypotonic medium in the presence or absence of IBTX (50 nM). Figure 3-3B demonstrates that maximum cell volume increase was observed in the presence of IBTX. Additionally, IBTX inhibited the regulatory volume decrease and allowed for a sustained increase in cell volume in response to hypotonicity when compared to cells that were not treated with IBTX.

Exposure of TM cells to hypertonic medium resulted in a 31 % decrease in cell volume. Hypertonic medium was then exchanged with isotonic medium at 37^{o}C in 5% CO_2 after which cell volume increased (Figure 3-3B).

The NO-induced Decrease in Cell Volume Involves Activation of sGC and cGMP

To test the involvement of sGC in the NO-induced decreases in cell volume, primary human TM cells (HTM44 and HTM86) were incubated with Calcein AM as described above. Images were taken at 0 time point, without drug, then DETA-NO (100 μM) was added to the

cells in the presence or absence of ODQ (1 μM) [73] , the specific sGC inhibitor, and images were taken at 5, 10, 15 and 20 min time points. Figures 3-4A and B demonstrate that ODQ abolished the NO-induced decreases in cell volume in both human and porcine TM cells. As with primary human TM cells (Figure 3-4A), decreases in cell volume in response to DETA-NO in porcine TM cells are also time-dependent (Figure 3-4B). ODQ (1 μM) abolished this time-dependent decrease in TM cell volume suggesting that the NO-induced decreases are mediated by sGC and cGMP.

Involvement of Protein Kinase G in the NO-Induced Decreases in TM Cell Volume

The pathway downstream of sGC was tested using the cGMP analog, 8-Br-cGMP. Primary human TM cells (HTM86, HTM44) were incubated with 8-Br-cGMP (2 mM) [74] and cell volume was determined. Figure 1-5 demonstrates that as with DETA-NO, 8-bromo-cGMP significantly reduced TM cell volume suggesting the involvement of cGMP and possible involvement of protein kinase G in regulating TM cell volume. To further determine if protein kinase G is involved in the NO-induced decreases in TM cell volume, human TM cells (HTM26, HTM86) were incubated with DETA-NO (100 μM) or 8-Br-cGMP (2 mM) [75] with or without the specific inhibitor of protein kinase G, (RP)-8-Br-PET-cGMP-S (50 μM) [76] . Figure 5 shows that (RP)-8-Br-PET-cGMP-S partially inhibited the DETA-NO- and 8-Br-cGMP- induced decreases in TM cell volume suggesting a role for protein kinase G in regulating cell volume.

BK_{Ca} Channels are Involved in the NO-Induced Decreases in TM Cell Volume

To test whether or not activation of the BK_{Ca} channel was involved in the NO-induced decreases in cell volume, HTM cells (26 and 80) were pre-incubated with IBTX (100 nM), and images were captured at 0 time point. DETA-NO (100 μM) was then added to the cells and images were captured at 5, 10, 15, 20 minutes time period post DETA-NO exposure. Figure 3-6

(open circles) demonstrates that NO was unable to cause decreases in TM cell volume in cells that were pretreated with IBTX. We next wanted to determine the effects of IBTX on cells that had experienced decreased cell volume in response to NO treatment. Images were captured without drugs at 0 time point. Cells were then treated with DETA-NO (100 μM) and images were captured at 5, 10 and 15 minutes. IBTX (100 nM) was then added at 15 minutes post DETA-NO treatment and images were captured at 20 minute time point. Figure 3-6 demonstrates that decreases in cell volume were time-dependent, with significant decreases observed at 10 and 15 minutes post drug incubation. Addition of IBTX 15 minutes post incubation with DETA-NO, reduced the NO-induced decreases in cell volume when compared with only DETA-NO treated cells. Additionally, IBTX alone had no significant effect on HTM cell volume (Figure 3-6).

Discussion

In this study we provide evidence that NO decreases TM cell volume by activation of the sGC/cGMP/PKG pathway in a manner dependent on BKCa channels (Figure 3-7). We also show that the time course for increased outflow facility in response to NO correlates with changes in cell volume in response to NO.

Outflow Facility

In our experimental protocol an acute application of DETA-NO increased outflow facility in porcine eye anterior segments. Other studies in monkeys [77] and rabbits [61] demonstrate the involvement of the NO/sGC and cGMP pathway in increasing outflow facility. The NO-effect was immediate, transient and the degree of increases in outflow facility varied among experiments. We do not know the reason for this variability in response to NO. The possibility exists that lower flow rates allow for increased time for medium to be held in the anterior segment of the eye, thus bathing the tissue with the drug for a longer period of time, hence

producing a more sustained drug effect. The ability of NO to increase outflow facility is corroborated by reports from Kotikoski et al. demonstrating the ability of NO donors to increase outflow facility in rabbit eyes [61] .

Additionally, we demonstrated the ability of IBTX to inhibit the NO-induced increases in outflow facility. The rapid reversal of the NO-induced increases in outflow facility by IBTX would suggest that inhibition of the BKCa channel would possibly stop cell shrinkage and allow for a rapid regulatory volume increase. Other studies have demonstrated that the BKCa channels are downstream effectors of NO and are involved in mediating the NO/cGMP-induced smooth muscle relaxation [78] . In TM, the BKCa channel is expressed and is involved in the NO-induced relaxation of precontracted bovine TM muscle strips [25] . These data suggest that in addition to its ability to regulate the NO-induced decreases in cell volume, the BKCa channel may be involved in regulating the contractile states of cells in the outflow pathway. In physiological states, NO could cause previously contracted cells to relax thus increasing outflow facility. Blocking the BKCa channel would potentially cause the cells to contract, thus causing outflow facility to return to base line values. Taken together these data suggest the possible involvement of both NO-induced decreases in cell volume and/or changes in the cells contractile states as cellular functions by which TM cells are altered.

The proposed role of NO in regulating IOP is not without controversy, however. One report by Krupin et al demonstrated an increase in IOP in rabbits in response to the NO donor sodium nitroprusside [79] . While we do not understand the reason for this discrepancy is is possibly explained by dose-dependent effects of NO on IOP. Higher doses of NO donors result in increases in IOP, while lower doses result in decreases in IOP [59, 80] . Additionally, repeated

use of the organic nitrate, nitroglycerin, resulted in tolerance, where as chronic usage of the nucleophile, hydralazine, did not result in tolerance [59] .

Increases in the osmolarity of the perfusion medium resulted in increases in outflow facility which mimicked the effects of DETA-NO. Consistent with the literature, anterior eye segments perfused with hypertonic medium [7, 48] resulted in increases in outflow facility while hypotonic medium [5, 7, 48] resulted in decreases in outflow facility.

Cell Volume Studies

Our protocol allowed us to quantify changes in cell volume in hundreds of intact, adherent cells in their native states and each cell was able to serve as its own control. While we allowed for Calcein AM to achieve a stable baseline after which cell volume was measured in response to drug treatment in isotonic medium, we also imaged cells that were not treated with drugs to assess any changes in fluorescence in response to laser exposure. Additionally, because during the experimental protocol these cells were in their native state and were not harvested, we did not experience the movement of cells from the region of study or observe the rapid contraction and relaxation phenomenon as previously described [4, 81] .

It has been observed that TM cell culture contains two distinct cell populations [39, 82] which is consistent with the identified regions of the TM, the cribriform or juxtacanalicular region, the uveal and the corneoscleral regions [3, 38] . In our hands we were able to visually identify the different cell types, however, as with reports by Mitchell et al [36] all cells that were analyzed did not experience decreases in cell volume in response to drug treatment. The juxtacanalicular region, and hence the juxtacanalicular cells are regions of high resistance to aqueous humor outflow and may constitute the area where changes in cell volume may affect outflow resistance. Together, these data would suggest that modulation of the volume of TM cells may modify outflow resistance of aqueous humor, and may alter IOP.

We tested the validity of our protocol with agents and conditions known to alter the osmolarity of the medium and subsequently alter TM cell volume. Both swelling and shrinkage of TM cell after exposure to hypotonic or hypertonic media respectively demonstrated that TM cells have the ability to respond to osmotic changes in their extracellular environment. Our initial studies were performed in porcine cells where we observed that increases in cell volume were detectable at 1 minutes post osmotic changes and cell volume decreased within 3 minutes post hypotonic exposure.

Porcine cell volume in response to hypertonic changes decreased gradually over a 7.5 minute period and remained constant for the duration of the experiment. Because of these observations we performed similar experiments in human TM cell. Cell volume changes in response to hypotonic treatment mimicked the hypotonic effects observed in porcine TM cell line.

Exposure of TM cells to hypotonic medium resulted in 11 % increase in cell volume. These results mimic similarly treated TM cells [36, 49] . To date the correlation between amount of changes in cell volume in response to changes in osmolarity or drugs and the physiological relevance of these changes to cell function has not been ascertained. As with these studies, other studies by Mitchell et al, demonstrated that human TM cells exposed to hypotonic solution experienced regulatory volume decrease within 4 minutes of treatment with hypotonic medium [4] . In our experimental protocols neither porcine nor human cells treated with mannitol or NaCl experienced regulatory volume increase in the presence of hypertonic medium. Immediate regulatory volume increase was observed when hypertonic medium was exchanged with isotonic medium at 37° C [6] with cell volume restored to baseline values within 6 minutes of medium exchange.

In our hands, TM cells exposed to hypotonic medium experienced a peak cell volume increase when treated with IBTX. This suggests that in physiological states the BKCa channel may be involved in the regulatory volume decrease mechanism in the cell inhibition of which may potentiate cell swelling. IBTX abolished the regulatory volume decrease that occurred spontaneously in hypotonic treated cells suggesting a role for the BKCa channel in the cells regulatory volume decrease mechanism.

NO donors can activate sGC in a number of tissues, presumably through release of NO. The ability of the specific sGC inhibitor ODQ to antagonize the actions of DETA-NO on TM cell volume would suggest that a direct consequence of NO stimulation is the activation of sGC. Technical constraints did not allow us to correlate changes in endogenous cGMP levels with changes in TM cell volume. However, 8-Br-cGMP mimicked the actions of DETA-NO suggesting that cGMP is involved in TM cell volume regulation. In fact our studies involving 8-Br-cGMP corroborated previous results published by O'Donnell et al. In these studies exposure of bovine TM cells to 8-Br-cGMP (50 μM) resulted in an 8% decrease in TM cell volume [6] . These studies were performed using electronic cell sizing of suspended TM cells. Similar changes in cell volume were observed in human TM cells in our experiments using fluorescent probes validating our protocol.

In other studies, exposure of TM cells to 8-Br-cGMP (50 μM) resulted in inhibition of the bumetanide-sensitive K+ influx demonstrating the involvement of cGMP in the Na-K-2Cl co-transport regulation [6] . In our hands, the decreases in TM cell volume in response to DETA-NO were similar to decreases in cell volume in response to 8-Br-cGMP suggesting that cGMP maybe the second messenger mediating the effects of NO on cell volume. Our studies demonstrated that IBTX inhibited the NO-induced decreases in TM cell volume suggesting the involvement of

the BKCa channel and K+ efflux in regulating the NO-induced decreases in TM cell volume. We also demonstrated that BKCa channel is necessary for the NO-induced response in TM cells. Other studies demonstrated that cGMP generated by activation of the atrial natriuretic peptide receptor, and by the NO donor, sodium nitroprusside, decreased cardiac cell volume by inhibiting ion uptake by the Na-K-2Cl co-transporter [83] . These observations suggest that NO regulation of K+ transport and cell volume are bidirectional, facilitating both K+ efflux via BKCa channel and K+ influx via bumetanide-sensitive K+ cotransporter.

Protein kinase G inhibitors were able to inhibit the NO- and 8-Br-cGMP-induced changes, demonstrating the role of protein kinase G and protein phosphorylation events in regulating TM cell volume. Our studies, however, do not preclude the involvement of other second messengers, including cAMP [49, 84] , or protein kinase C [85] or the involvement of other ion transporters and co- transporters in modulating cell volume [4] .

We were not able to demonstrate that the NO-induced increases in outflow facility occurred as a result of changes in TM cell volume. However, we have demonstrated that the time course for the DETA-NO induced increases in outflow facility correlate with the time course for the DETA-NO-induced decreases in cell volume. Changes in TM cell volume induced by changes in tonicity correlate with tonicity-induced changes in outflow facility. Studies have demonstrated that drugs known to cause cell swelling reduce outflow facility while drugs know to shrink cells increase outflow facility in human and bovine eyes [5, 7] . While the results of a study by Gabelt et al., demonstrated that bumetanide, an inhibitor of the Na-K-2Cl co-transporter had no effect on outflow facility in living primate eyes (suggesting that alterations in cell volume had no effect on outflow facility) [86] , the preponderance of electrophysiological, biochemical and pharmacological studies demonstrate a correlation between cell volume changes

and outflow facility. Together, these studies suggest that there might be multiple transporters involved in cell volume regulation and subsequent regulation of outflow facility.

We conclude that NO decreases TM cell volume, that cellular response to NO is mediated by sGC, cGMP, PKG and BKCa channels, and that changes in cellular volume are correlated with changes in outflow facility. We are mindful that there might not be a direct cause and effect relationship between TM cell size and outflow facility because we have not accounted for possible involvement of TM contractile mechanisms [50-52]

Acknowledgements

We thank Drs. T. Acott and D. Stamer for teaching us the anterior segment organ perfusion protocol and TM cell culture techniques, Mr. Douglas Smith for technical assistance with the Confocal Microscope and Drs. Charles Wood and Elaine Summer for helpful discussion of the manuscript.

Grant

This work was supported by a grant from the American Health Assistance Foundation, National Glaucoma Research.

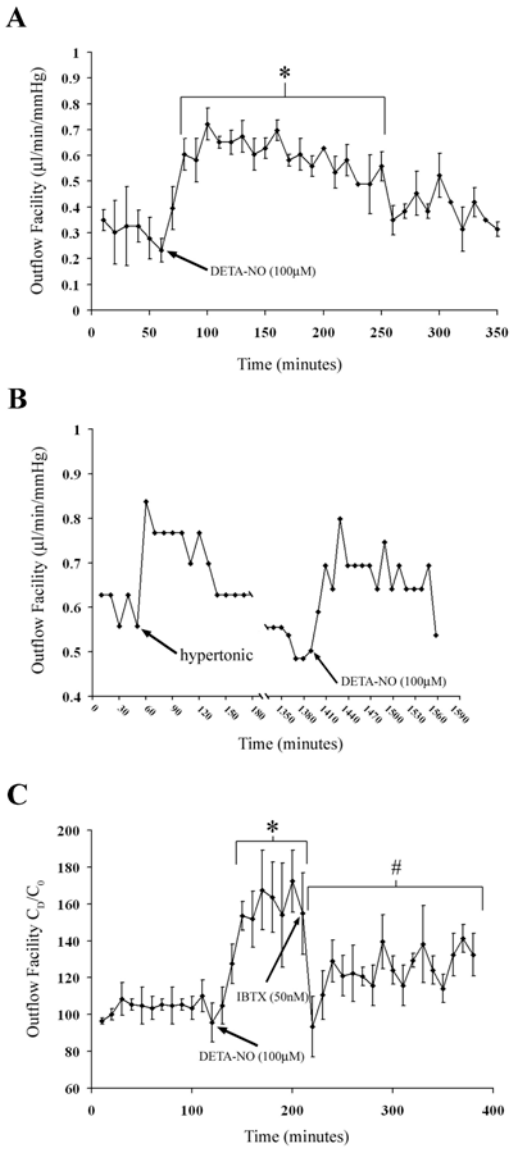

Figure 3-1. NO donors increase outflow facility in porcine anterior organ culture perfusion. A) A stable baseline was achieved after which the anterior chamber perfusate was replaced with an acute treatment of DETA-NO (100µM) dissolved in DMEM. The drug entry port was clamped, and perfusion continued with DMEM alone. Data shown is representative of 8 experiments. *Significantly different from baseline values at 30 and 50 minutes, $P<0.05$; ANOVA and the Holm-Sidak method. B) A stable baseline was achieved after which the isotonic medium was exchanged with hypertonic DMEM. Following the effects of the hypertonic DMEM, a stable baseline was reestablished and DETA-NO (100µM) was then added to the perfusate. Data shown is representative of 3 experiments. C. A stable baseline was established and anterior eye segment was perfused with DETA-NO (100µM). Subsequently, IBTX (50 nM) was added to the perfusate. Data shown is representative of 3 experiments. *Significantly different from baseline at 50 and 100 minutes and # significantly different from DETA-NO treated samples $P<0.05$; ANOVA and the Holm-Sidak method.

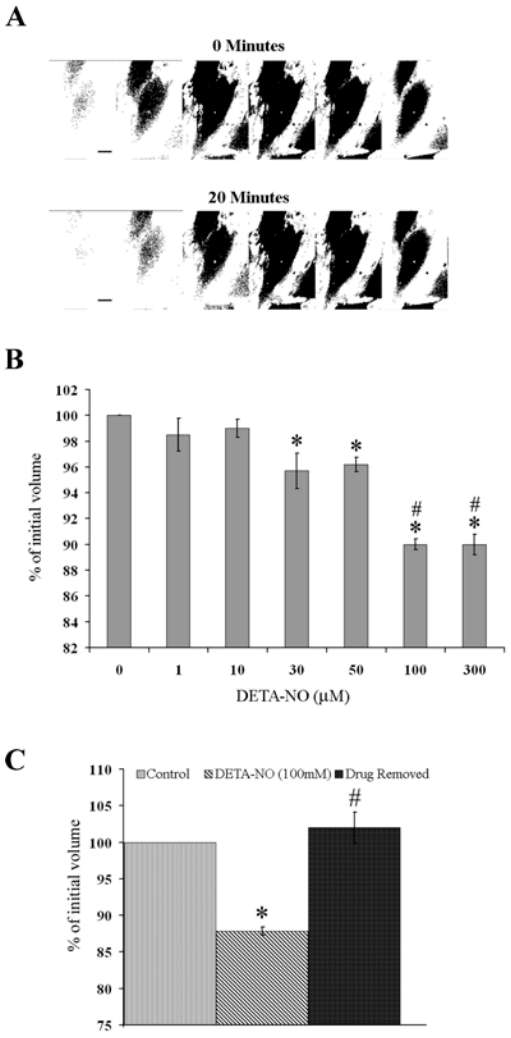

Figure 3-2. NO decreases TM cell volume. A) Thresholded z-stack images of a TM cell. At 0 minutes (without drug), the thresholded voxels are qualitatively and quantitatively greater than at 20 minutes post DETA-NO (100 μM) treatment. Voxel count for cell at 0 minute, 27650 and at 20 minutes, 23342. Scale bar = 20μm. B) NO-induced decreases in cell volume are concentration-dependent. Confocal images of the same cells were acquired with a 20x objective lens at 1μm z-step intervals to a depth of 15 μm. Human TM cells were exposed to varying concentrations of DETA-NO (1 – 300 μM). Images were captured at 0 and 20 minute time points. Data shown for 1, 10, 30, 50, 100 and 300 μM DETA-NO represent the mean $\pm$ SEM for 23, 31, 19, 22, 44 and 23 cells respectively and are expressed as % of initial volume at 0 time point without drugs. Average voxel count is 25,449 + 4398 (*Significantly different from control . $P<0.05$; # significantly different from 30 and 50 μM DETA-NO, $P<0.05$; ANOVA and the Holm-Sidak method). 2C). Decreases in human TM cell volume are reversible.. Data are expressed as % of initial volume at 0 time point mean ± SEM; n=23 cells. Voxel count for 0 time point is 11606 $\pm$ 1155 (*Significantly different from control (0 time point) $P<0.001$, # significantly different from DETA- NO treated cells $P<0.05$).

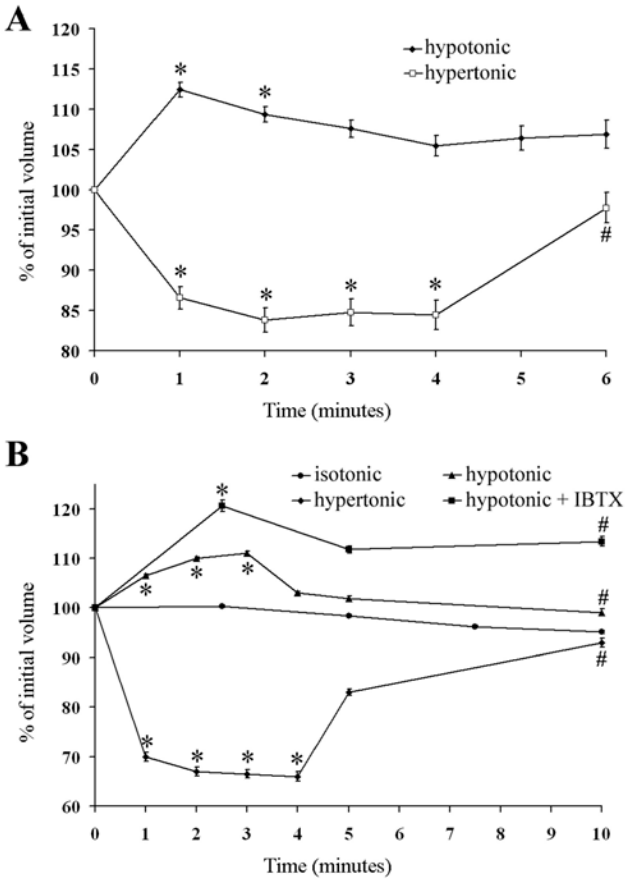

Figure 3-3. Changes in osmolarity effect changes in TM cell volume. A) In porcine TM cells hypotonic DMEM increased cell volume (mean ± SEM; n=55 cells) and hypertonic DMEM decreased cell volume (mean ± SEM; n= 47 cells). Data are expressed as % volume at 0 time point. Voxel count at 0 time point for hypotonic treatment 2385.1+ 290 (*significantly different from 0 time point, $P<0.05$ and # significantly different from 1,2,3 and 4 min $P<0.05$). Voxel count for hypertonic treatment 2827.5 + 274 (*significantly different from 0 time point $P<0.05$;). B) In human TM cells hypotonic DMEM increased cell volume (mean ± SEM; n=19 cells) while hypertonic DMEM decreased cell volume (mean ± SEM; n=17 cells). Hypotonic + IBTX allowed for a sustained increase in cell volume (mean + SEM; n=66 cells). There were no changes in cell volume in cells incubated in isotonic medium (mean + SEM; n=39 cells). Data are expressed as % volume at 0 time point. Voxel count at 0 time point for hypotonic, hypertonic, isotonic and hypotonic + IBTX treatments are 3273 + 533; 7921 + 1230; 4392 + 278; and 5408 + 286 respectively (* Significantly different from control (0 time point) and # significantly different from anisosmotic treated cells, $P<0.05$; ANOVA and the Holm-Sidak method.

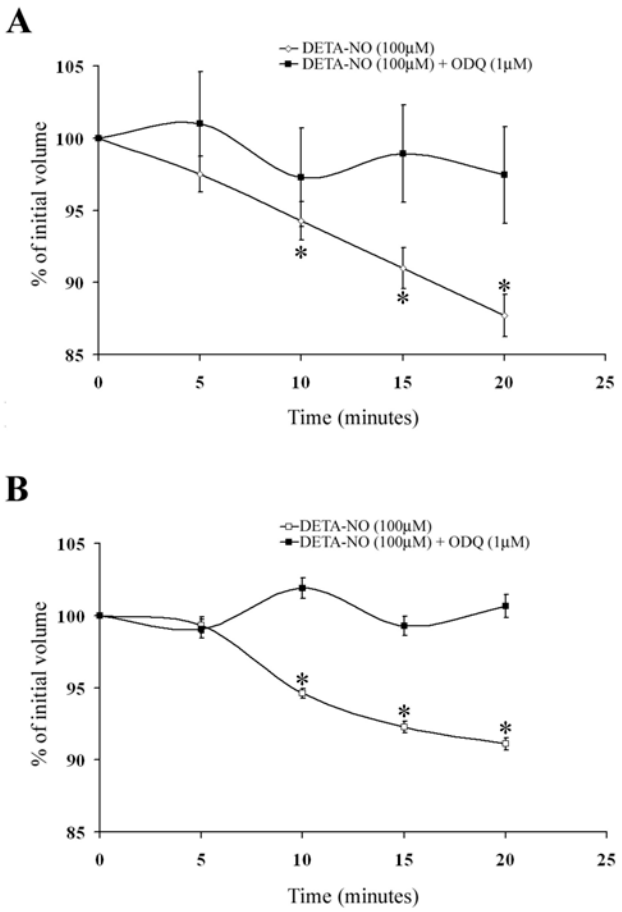

Figure 3-4. sGC mediates the NO-induced decreases in TM cell volume. A). Data are expressed as % of initial volume at 0 time point and for: DETA-NO treated group represents the mean ± SEM; n=28 cells and for DETA-NO + ODQ- treated group represents the mean ± SEM; n=33 cells. Voxel count for 0 time point: DETA-NO, 16855 $\pm$ 3185; DETA-NO + ODQ, 11923 $\pm$ 908 (* Significantly different from 0 time point $P<0.001$). B) As with human TM cells, porcine TM cells were exposed to DETA-NO and ODQ as described. Data are expressed as % of initial volume at 0 time point and for DETA-NO- treated group represents the mean ± SEM; n=111 cells and for DETA-NO + ODQ- treated group represents the mean ± SEM; n=11 cells. Voxel count for 0 time point: DETA-NO, 2994 $\pm$ 171; DETA-NO + ODQ, 2288 $\pm$ 81 (* Significantly different from 0 time point $P<0.001$).

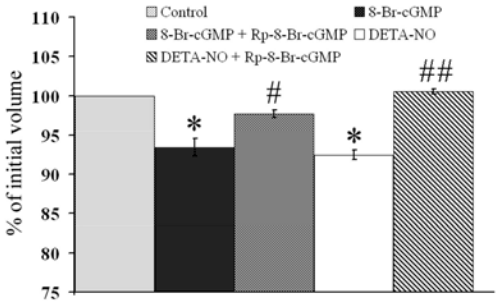

Figure 3-5. Effects of PKG inhibitor (RP)-8-Br-PET-cGMP-S (PKGi) on 8-Br-cGMP- and DETA-NO- induced decreases in TM cell volume. Cells were incubated with 8-Br-cGMP (2 mM) or DETA-NO (100 μM) in the presence or absence of (RP)-8-Br-PET-cGMP-S (50 μM). Images were taken and cell volume measured. Data are expressed as % of initial volume at 0 time point and represents the mean ± SEM for: 8-Br-cGMP, n=100 cells; 8-Br-cGMP+PKGi, n=86 cells; DETA-NO mean ± SEM, n=89 cells; DETA-NO + PKGi mean ± SEM, n= 97 cells. Voxel count for 0 time point: 8-Br-cGMP, 2771± 102; 8-Br-cGMP + PKGi, is 4742 ± 155; DETA-NO-, 4125 ± 123; DETA-NO + PKGi, 3422 ± 131. * Significantly different from 0 time point and # significantly different from 8-Br-cGMP group $P<0.001$ and ## significantly different from DETA-NO treated cells $P<0.001$.

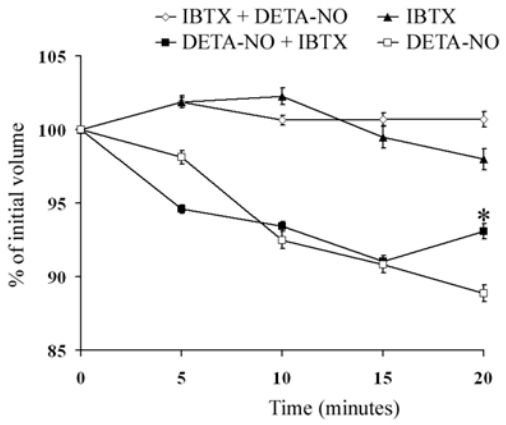

Figure 3-6. BK_{Ca} channels mediate the NO-induced decreases in TM cell volume. IBTX only: data are expressed as % of initial volume at 0 time point and represents the mean ± SEM; n= 58 cells. DETA-NO + IBTX: images were captured at 0 time point without drugs, then DETA-NO (100 μM) was added and images were captured at 5, 10 and 15 minutes. IBTX (100 nM) was added at 15 minutes and images were taken at 20 minutes. DETA-NO: cells were incubated with DETA-NO only and data at 20 minute time point was compared with data obtained at 20 minute time point for the DETA-NO + IBTX treated cells. Data are expressed as % of initial volume at 0 time point and represents the mean ± SEM; n= 46 cells. * DETA-NO + IBTX was significantly different from DETA-NO treated cells $P<0.05$. IBTX + DETA-NO: TM cells were pre-incubated with IBTX then images were captured. The cells were then exposed to DETA-NO (100 μM) and images were captured at 5, 10, 15 and 20 minutes. Data are expressed as % of initial volume at 0 time point and represents the mean ± SEM; n= 51 cells. Voxel count for 0 time point: IBTX, 13147 ± 865; DETA-NO + IBTX, 9202 ± 625; IBTX + DETA-NO, 19202 ± 925.

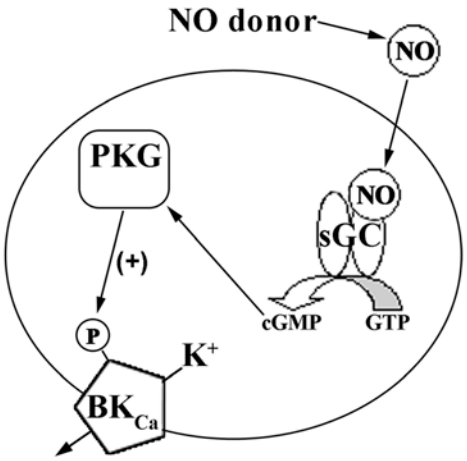

Figure 3-7. Summary diagram of the pathway of NO regulation of TM cell volume. NO donors cause the formation of NO, which then binds to and activates soluble guanylate cyclase (sGC), the synthetic enzyme of cGMP. cGMP and its analogue 8-Br-cGMP activate protein kinase G (PKG) which may, directly or indirectly phosphorylate BKCa channels, with subsequent K+ efflux and decreases in cell volume.

CHAPTER 4
HUMAN TRABECULAR MESHWORK CELL VOLUME DECREASE BY NO-INDEPENDENT SOLUBLE GUANYLATE CYCLASE ACTIVATOR YC-1 AND BAY-58-2667 INVOLVE THE BK_{CA} ION CHANNEL

Introduction

Aqueous humor exits the eye through the TM and Schlemm's canal. Activation of sGC by NO -dependent donors increase the rate at which aqueous humor flows through the TM and Schlemm's canal. These changes in outflow facility occur concomitant with sGC- induced decreases in TM cell volume. Soluble guanylate cyclase comprises an α subunit and a smaller heme-containing β subunit [87, 88] , both of which constitute the active enzyme. Heterodimers are activated by NO binding to the heme moiety, whereas homodimers exhibit little or no synthetic activity, even in the presence of the ligand. Binding of NO to sGC, results in the formation of 3',5'-cyclic guanosine monophosphate (cGMP) from guanosine 5'-triphosphate (GTP). Increased cGMP activates protein kinase G (PKG) [89] , with subsequent phosphorylation of target proteins.

NO acting through the sGC, cGMP and PKG pathway decreased TM cell volume in a time course that correlated with the NO-induced increases in outflow facility in perfused eye anterior segments [90] . Although NO is a potent regulator of IOP, chronic administration of NO-donors to eyes result in lack of responsiveness and the development of tolerance [59] . Therefore, the need to identify other activators of sGC that regulate TM cell function is of vital interest. YC-1 [3-(5'-hydroxymethyl-2'furyl)-1-benzyl indazole) [18] , a benzyl indazole derivative, and BAY-58-2667 [91] are NO-independent activators of sGC. As with NO activation of sGC, YC-1 and BAY-58-2667 activation of sGC also results in increases in cGMP and PKG phosphorylation events.

Alterations of the contractile states and volume of the TM cells would regulate aqueous humor outflow [5-7, 43-49] . Changes in cell volume are influenced by the activities of the Na-K-2Cl

co-transporter [6, 7, 36] the Na+/H+ transporter [36] , the K+ and Cl- channels [5, 36] and the large conductance calcium-activated potassium channel (BK_{Ca}) [90] . Further, it is possible that both the cellular contractile mechanisms and the cell volume regulatory mechanisms are functionally linked [50-52] ; as the BK_{Ca} channels have been shown to regulate TM cell volume and contractility [5, 45] and outflow facility [5] . In these studies we will test the hypothesis that YC-1 and BAY-58-2667 regulate TM cell function. Specifically, we will test the ability of YC-1 and BAY-58-2667 to regulate TM cell volume, and test the involvement of sGC, cGMP, PKG and BK_{Ca} channel in the YC-1 and BAY-58-2667 induced response.

Materials and Methods

Cell Culture

Eyes from human donors with no history of ocular disease or surgery were obtained from Lions Eye Institute (Tampa, FL) within 24-30 hours postmortem. Primary human TM cell lines (numbers representing ages of the donors) (HTM26, HTM71, HTM36, HTM80 and HTM86) were developed. For our experimental protocols cells from early passages (3-5) were used. Human TM explants were obtained either from whole eyes that were stored in a moist environment at 4^{o}C or from corneal scleral rims stored in Optisol (Dexol; Chiron Ophthalmics, Irvine, CA) at 4^{o}C. TM cells were isolated after collagenase digestion of TM explants [64] . Collagenase-treated cells were grown in low glucose (1g/L) DMEM (Mediatech, Herdon VA.) in the presence of 10% fetal bovine serum (Mediatech, Herdon VA.), 100 U/ml penicillin and 100 μg/ml streptomycin (Mediatech, Herdon VA.) and then passaged into 6-well culture dishes (Nalge Nunc International, Rochester, NY) in a tissue culture incubator @ 37^{o}C in 5% CO_2. We validated human TM cells by their morphology and the presence of dexamethasone-induced myocillin expression [33] . For experimental protocols, TM cells were grown on Lab-Tek ll chambered cover glass (Nalge Nunc International, Rochester, NY) in low-glucose DMEM as

described above to 100% confluency, after which they were exposed to serum free media for 2 days prior to performing the experiments.

Measurement of Cell Volume

Cell volume measurements were performed as previously described [90] . Prior to any drug treatments, the cells were loaded with the fluorescent dye Calcein AM (2 μM) in DMEM at 37°C, in 5% CO_2 incubator for 60 minutes to ensure a stable baseline. The coverslips containing the cells were subjected to confocal microscopy using a Leica confocal microscope, thermostated at 37^{o}C and images of the same cells were acquired with a 20x objective lens at 1μm z-step intervals to a depth of 15 μm. Because during the experimental protocol these cells were in their native state and were not harvested, we did not experience the movement of cells from the region of study or observe the rapid contraction and relaxation phenomenon as previously described [36, 81] .The confocal microscope calculated the number of voxels and cell volume was quantified using NIH ImageJ software. The NIH ImageJ software was used to identify the top and bottom edges of the cell. Images were converted from 8-bit to binary values using a threshold that was determined by analysis of fluorescent Fluoresbrite latex beads (Polyscience Inc., Warrington) of known diameter and volume that were imaged under conditions identical to those used for TM cells. A region of interest was then selected around each cell and the ImageJ software was used to calculate the number of voxels in the region of interest in the image stack. Changes in cell volume were determined by dividing the voxel count with drug treatment by the voxel count without drug treatment. Unless otherwise stated in the text, for studies involving drug treatments, images were taken without drug treatment (0) time point which served as controls for the treatment groups. Because our preliminary data demonstrated that the maximum decrease in TM cell volume in response to drug treatment was achieved at 20 minutes, images were taken of the

same cells at 20 minutes post drug-treatment. For all experiments, YC-1 (10 mM) and BAY-58-2667 (10 mM) were solublized in a DMSO-ethanol mixture for a final concentration of 0.1%.

cGMP Assay

For cGMP measurements, cells were grown in 12-well culture dishes (Nalge Nunc International, Rochester, NY) in a tissue culture incubator @ 37^{o}C in 5% CO_2 as described above. Two days prior to experiments, the cells were exposed to serum-free media. Cyclic GMP was assayed by an Enzyme Immuno Assay (EIA) (Amersham Biosciences, Piscataway, NJ) according to the manufacture's protocol.

Materials and Reagents

Routine reagents, YC-1 [3-(5'-hydroxymethyl-2'furyl)-1-benzyl indazole) and iberiotoxin (IBTX) were purchased from Sigma (St. Louis, MO). Others were obtained as follows: 8-bromo-cGMP sodium salt, 1*H*-[1,2,4]oxadiazolo[4,3-a]quinoxalin-1-one (ODQ), from Sigma-RBI (Natick, MA); (RP)-8-Br-PET-cGMP-S from Calbiochem (La Jolla, CA). Bay-58-2667 was obtained from Alcon Research, Ltd.,(Fort Worth, TX).

Statistics

Statistical comparisons were performed by ANOVA, followed by Holm-Sidak method or Fisher LSD method for comparison of significant difference among different means.

Results

YC-1 and BAY-58-2667 -Induced Regulation of TM cell Volume are Biphasic

To quantitatively measure changes in cell volume, HTM36 and HTM80 cells were exposed to varying concentrations of YC-1 (10 nM - 200 μM) [92] . Figure 4-1A demonstrates that the action of YC-1 is biphasic in HTM cells; 1 μM significantly increased TM cell volume while higher concentrations (50 – 200 μM) decreased TM cell volume. We also observed that there were no changes in cell volume over time in cells incubated in Calcein AM only (Figure 4-1A).

Similarly, varying concentrations of BAY-58-2667 (10 nM – 100 μM) were added to TM cells and images were captured with or without drugs. Figure 4-1B demonstrates that as with figure 4-1A, the action of BAY-58-2667 on TM cell volume is biphasic; 100 nM caused increases in TM cell volume, while higher concentrations resulted in decreases in TM cell volume.

The YC-1-induced Decrease in Cell Volume Involves Activation of Soluble Guanylate Cyclase and cGMP

To test the involvement of sGC in the YC-1-induced decreases in cell volume, primary human HTM36 and HTM80 cells were incubated with YC-1 (150 μM) in the presence or absence of ODQ (500 nM - 5 μM) [73] the specific sGC inhibitor, and images were taken at 20 min. ODQ at 500 nM and 1 μM had no effect on the YC-1- induced decreases in TM cell volume while 5 μM significantly attenuated the YC-1 effect (Figure 4-2A). Because activation of sGC results in increased cGMP levels, we examined the ability of exogenously applied cGMP to decrease TM cell volume. Figure 4-2A demonstrates that the non-hydrolyzable analog of cGMP, 8-bromo-cGMP, mimics the action of YC-1 in decreasing TM cell volume.

To further determine if sGC is involved in the YC-1-induced decreases in HTM cell volume, the ability of YC-1 (50 - 150 μM) to increase cGMP levels was tested. There was a concentration-dependent increase in cGMP levels in cells treated with varying concentrations of YC-1 that was saturating at 100 μM (Figure 4-2B). Additionally, ODQ (5μM) abolished the ability of YC-1 (150 μM) to increase cGMP levels (Figure 4-2B).

Unlike YC-1 however, ODQ (5 and 10 μM) potentiated the BAY-58-2667 –induced decreases in TM cell volume (Figure 4-2C). While we were unable to pharmacologically determine sGC involvement, we tested down-stream effects. Cyclic GMP levels were measured in high concentration-exposed BAY-58-2667 samples. Figure 4-2D demonstrates that BAY-58-

2667 (10 and 100 μM) increased cGMP levels. Similarly, 8-Br-cGMP mimicked the actions of BAY-58-2667 in decreasing TM cell volume (Figure 4-2C).

The YC-1 and BAY-58-2667-induced Increases in Cell Volume Do Not Involve cGMP

To determine if sGC is involved in the low concentration YC-1 and BAY-58-2667 induced increases in cell volume, HTM36 and HTM80 cells were incubated with Calcein AM then exposed to YC-1 (10 nM - 25 μM) and BAY-58-2667 (100 nM) and cGMP levels were then measured. Addition of 10 nM - 25 μM YC-1 to HTM cells did not result in a statistically significant increase in cGMP levels when compared to control samples (Figure 4-3A). There were no alterations in cGMP levels in TM cells incubated with YC-1 in the presence of ODQ (5 μM) (Figure 4-3A). Although it appears as if there is a trend for decreases in cGMP levels when ODQ (5 μM) was added in the presence of YC 1(1 μM), when all concentrations of YC 1 were included in the data analysis of the cGMP assay, the decrease was not statistically significant. As with low concentrations of YC-1, BAY-58-2667 (100 nM) did not result in a statistically significant increase in cGMP levels (Figure 4-3B).

PKG is Involved in the YC-1 and BAY-58-2667 -induced Decreases in TM Cell Volume

The pathway downstream of sGC was tested by exposure of HTM cells to varying concentrations of the PKG inhibitor, (RP)-8-Br-PET-cGMP-S (25 – 100 μM). HTM cells were incubated with YC-1 (150 μM) in the presence of (RP)-8-Br-PET-cGMP-S (25 - 100 μM) and imaged. Addition of (RP)-8-Br-PET-cGMP-S (50 and 100 μM) resulted in the attenuation of the YC-1 – induced decreases in TM cell volume (Figure 4-4A). TM cells were also exposed to BAY-58-2667 (10 μM) in the presence of varying PKG inhibitor concentrations (25 - 100 μM) that resulted in concentration-dependent attenuation of the BAY-58-2667 effect (Figure 4-4B).

This provides evidence for the involvement of protein phosphorylation in mediating the YC-1 and BAY-58-2667 -induced decreases in TM cell volume.

BK_{Ca} Channels are Involved in the YC-1 and BAY-58-2667 -induced Decreases in TM Cell Volume

To test if activation of the BK_{Ca} channel is obligatory for the YC-1 and BAY-58-2667 -induced decreases in TM cell volume, HTM cells were pre-incubated with IBTX (100 nM) [5, 25] and images were captured at 0 time point. YC-1 (150 μM) and BAY-58-2667 (10 μM) were then added to the cells and images were captured at 20 minutes post drug exposure. Figure 4-5 demonstrates that IBTX attenuated both the YC-1 and BAY-58-2667 -induced decreases in TM cell volume. Additionally, IBTX alone had no significant effect on HTM cell volume (Figure 4-5).

Discussion

In this study we provide evidence that YC-1 and BAY-58-2667, nitric oxide-independent sGC activators decrease human TM cell volume through the involvement of the BK_{Ca} channel. Specifically, YC-1 at concentrations of 50 – 200 μM and BAY-58-2667 at concentrations of 10-100 μM decreased TM cell volume and these decreases are mediated by the sGC/cGMP/PKG pathway in a manner dependent on the BK_{Ca} channel (Figure 4-6). The actions of YC-1, however, are biphasic, with 1 μM causing increases in TM cell volume, while higher YC-1 concentrations elicit a cell volume reduction. As with YC-1, BAY-58-2667, at higher concentrations (10 μM -100 μM) significantly decreased TM cell volume while exposure to BAY-58-2667 (100 nM) resulted in a significant increase in cell volume. The data observed at the concentrations used are consistent with the know potency of YC-1 and BAY-58-2667; as BAY-58-2667 has previously been shown to have higher potency than YC-1 in activating sGC [93]. The biphasic effects of YC-1 and BAY-58-2667 could be explained by the possible existence of

two binding sites for these compounds on sGC that may involve heme-dependent and independent moieties of the sGC [91] .

Cell volume was measured in adherent cells in their native states and each cell was able to serve as its own control. After Calcein AM dye achieved a stable baseline, cell volume was measured in response to drug treatment in isotonic media. Additionally, cells that were not treated with drugs were also imaged to assess any changes in fluorescence in response to laser exposure. It has been observed that TM cell cultures contain two distinct cell populations [82] which is consistent with the identified regions of the TM, the cribriform or juxtacanalicular region and the uveal\corneoscleral region [3, 38] . The juxtacanalicular region, and hence the juxtacanalicular cells are regions of high resistance to aqueous humor outflow. While the cells in the juxtacanalicular tissue contribute very little to total tissue volume, the changes in cell volume in this area may have a large contribution to outflow resistance. While we were able to visually identify the two cell populations, we were unable to determine if the two cell populations respond to low or high YC-1 or BAY-58-2667 concentrations similarly.

The ability of the specific sGC inhibitor, ODQ, to antagonize the actions of YC-1 on TM cell volume would suggest that a direct consequence of YC-1 stimulation is the activation of sGC. We measured alterations in cGMP levels in response to varying concentrations of YC-1 and demonstrated a concentration-dependent increase in cGMP levels. Higher concentrations of YC-1 caused significant increases in cGMP levels that correlated with decreases in TM cell volume; however, increased cell volume in response to 1 μM YC-1 is cGMP-independent. The physiological and pharmacological significance of this observation is unclear at present. ODQ abolished the YC-1 –induced increases in cGMP, but had no effect on basal cGMP levels suggesting that ODQ acts by inhibiting the interaction of YC-1 with sGC. Further evidence for

the involvement of cGMP in the YC-1-induced response was demonstrated by the ability of 8-Br-cGMP to mimic the actions of YC-1 in decreasing TM cell volume. In our hands, the decreases in TM cell volume in response to YC-1 were similar to decreases in cell volume in response to 8-Br-cGMP suggesting that cGMP maybe the second messenger mediating the effects of YC-1 on cell volume.

Unlike ODQ's attenuation of the YC-1-induced decreases in TM cell volume, ODQ potentiated the BAY-58-2667 effects. While the precise mechanisms are unclear, experimental evidence suggests that removal of the heme prosthetic group or oxidation to its ferric form by ODQ causes conformational changes in sGC such that it no longer responds to NO or YC-1 but does respond to BAY-58-2667 [94] . While we did not demonstrate sGC involvement in the BAY-58-2667-induced decreases in TM cell volume, other studies have demonstrated that BAY-58-2667 binds to and activates sGC with subsequent increases in cGMP levels [93] . Similarly, we demonstrated that higher concentrations of BAY-58-2667 caused increases in cGMP levels that correlated with decreases in TM cell volume.

Additionally, the PKG inhibitor was able to inhibit both the YC-1and BAY-58-2667-induced cell volume changes, further demonstrating the role of PKG and protein phosphorylation events in regulating TM cell volume. Our studies, however, do not preclude the involvement of other second messengers, including cAMP [49, 84] and protein kinase C [85] .

IBTX inhibited the YC-1 and BAY-58-2667-induced decreases in TM cell volume suggesting the involvement of the BK_{Ca} channel and also the role of K^+ efflux in regulating the YC-1 and BAY-58-2667-induced decreases in TM cell volume. Similar observations were made in studies involving TM cells treated with NO in the presence of IBTX; preincubation of TM cells with IBTX abolished the NO-induced decreases in TM cell volume, suggesting that the

BK_{Ca} channel is obligatory for the sGC/cGMP induced decreases in TM cell volume [90] . While we do not know the mechanism(s) by which the sGC/cGMP/PKG system regulates the BK_{Ca} channel, other studies demonstrate that PKG phosphorylation of the α subunit of the BK_{Ca} channel results in its activation [28, 29] . Thus, the possibility exists that YC-1 or BAY-58-2667 activation of PKG in TM cells could result in phosphorylation of BK_{Ca} channels and subsequent decreases in TM cell volume.

While this study suggests the involvement of the BK_{Ca} channel and K^+ efflux in the BAY-58-2667 and YC-1-induced decreases in TM cell volume, other studies have demonstrated that cell volume decrease is accompanied by both K^+ and Cl^- efflux [95] induced by activation of K^+ and Cl^- channels and/or K^+ and Cl^- symport. This suggests that K^+ efflux may initiate a parallel Cl^- efflux in TM cells. In other studies, exposure of TM cells to 8-Br-cGMP (50 μM) resulted in inhibition of the bumetanide-sensitive K^+ influx demonstrating the involvement of cGMP in Na-K-2Cl co-transport regulation [6] . This suggests that the Na-K-2Cl co-transporter may be regulated by YC-1 and BAY-58-2667. However, its ability to decrease TM cell volume is dependent on low bicarbonate levels [6, 36] or blockade of the Na/H exchanger [36] , experimental conditions that were not manipulated in these studies. Furthermore, increased cGMP levels resulting from both sGC and membrane guanylate cyclase activation resulted in decreased cardiac cell volume through inhibition of K^+ influx via the bumetanide-sensitive K^+ cotransporter [83] . These observations suggest that NO-dependent and NO-independent regulation of K^+ transport and cell volume are bidirectional; facilitating K^+ efflux via BK_{Ca} channel and inhibiting K^+ influx by the Na-K-2Cl co-transporter.

Additionally, the NO–dependent sGC/cGMP system plays an important role in regulating aqueous humor dynamics by regulating; aqueous humor production in the ciliary processes [96, 97]

and aqueous humor outflow via the TM/Schlemm's canal [90] with subsequent decreases in IOP [19, 59]. Therefore, these data would suggest that modulation of the volume of TM cells by YC-1 and BAY-58-2667 via the sGC/cGMP/PKG system may modify aqueous humor outflow resistance, and thus may alter IOP.

Funding

Supported in part by a grant from the American Health Assistance Foundation, National Glaucoma Research, and Alcon Research Laboratories, Ltd.

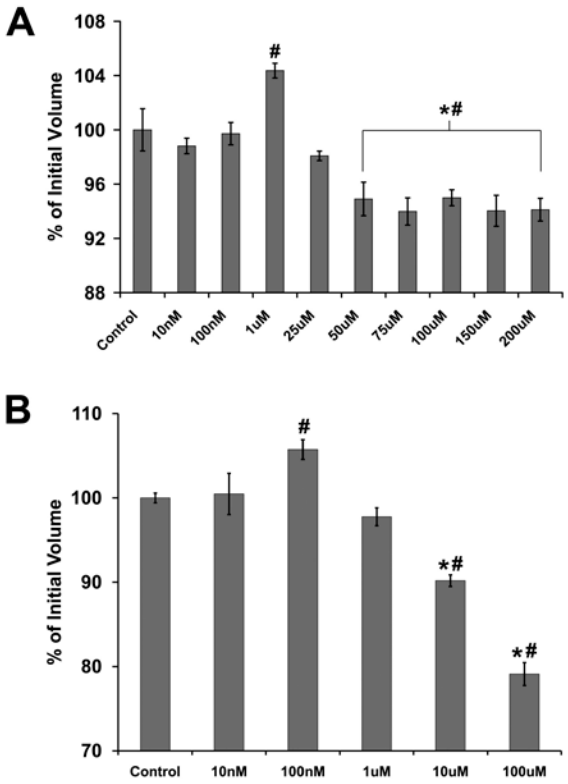

Figure 4-1. YC-1 and BAY-58-2667-induced regulation of TM cell volume is biphasic. A) YC-1-induced changes in cell volume are concentration-dependent. Human TM cells were exposed to varying concentrations of YC-1 (10 nM – 200 μM). Images were captured at 0 and 20 minute time points. Data shown represent the mean ± SEM for; control n=52 cells, 10 nM n=22 cells, 100 nM n=35 cells, 1 μM n=58 cells, 25 μM n=47 cells, 50 μM n=65 cells, 75 μM n=11 cells, 100 μM n=40 cells, 150 μM n=51 cells and 200 μM n=49 cells. Data are expressed as % of initial volume at 0 time point without drugs. #Significantly different from control at $P<0.05$; ANOVA and the Holm-Sidak method. *Significantly different from 1 μM YC-1 at $P<0.05$; ANOVA and the Holm-Sidak. B) Cells were exposed to varying concentrations of BAY-58-2667 (10 nM – 100 μM) and images were captured at 0 and 20 minutes. Data are expressed as % of initial volume at 0 time point without drugs and represent the mean ± SEM for; control n=22 cells, 10 nM n=26 cells, 100 nM n=17 cells ,1 μM n=17 cells, 10 μM n=13 cells and 100 μM n=17 cells. #Significantly different from control at $P<0.05$; ANOVA and the Holm-Sidak method. *Significantly different from 100 nM BAY-58-2667 at $P<0.05$; ANOVA and the Holm-Sidak.

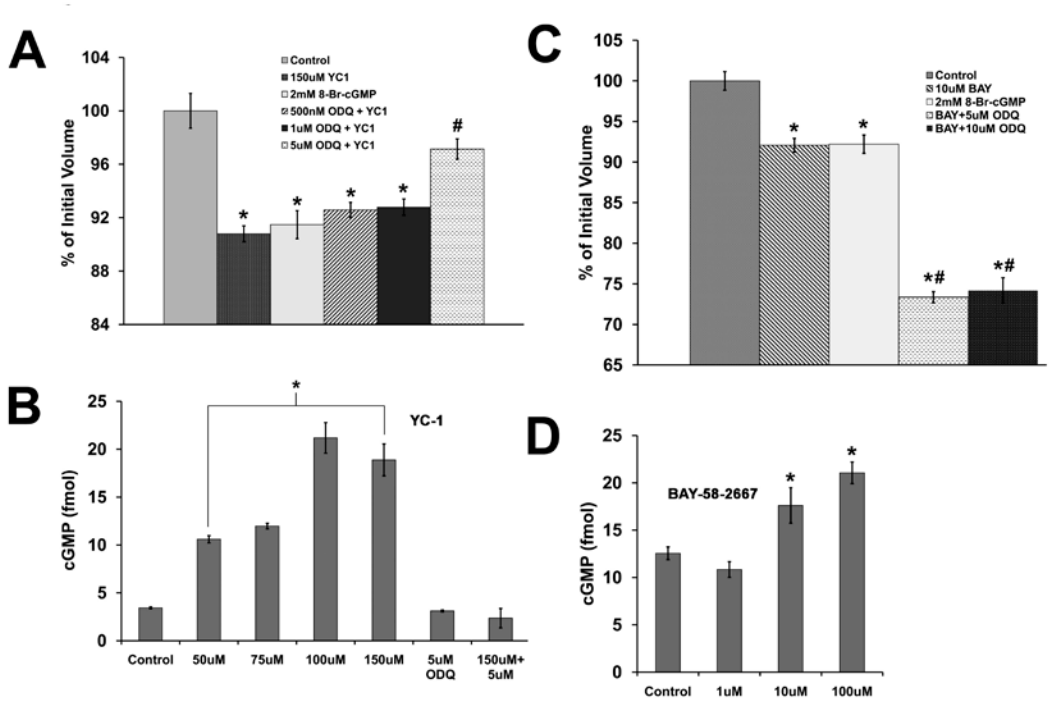

Figure 4-2. Involvement of sGC/cGMP in the YC-1 and BAY-58-2667-induced decrease in TM cell volume. A) ODQ inhibition of the YC-1–induced decrease in TM cell volume is concentration dependent. Data are expressed as % of initial volume at 0 time point and for: YC-1 (150 μM) treated group represents the mean ± SEM, n=24 cells; 8-Br-cGMP (2 mM) treated group represents the mean ± SEM, n= 71 cells; YC-1 + ODQ (500 nM) treated group represents the mean ± SEM, n=35 cells; YC-1 + ODQ (1 μM) treated group represents the mean ± SEM, n=31 cells; YC-1 + ODQ (5 μM) treated group represents the mean ± SEM, n=32 cells. *Significantly different from control at P<0.05; ANOVA and the Holm-Sidak method. #Significantly different from YC-1 (150 μM) treated group at P<0.05; ANOVA and the Holm-Sidak method. B) YC-1 - induced decrease in cell volume is associated with increases in cGMP. Levels of cGMP in TM cells after incubation with YC-1 (50 -150 μM) and YC-1 (150 μM) plus ODQ (5 μM). Results measured are expressed as mean ± SEM fmol of cGMP done in triplicate. *Significantly different from control at P<0.05; ANOVA and the Holm-Sidak method. C) ODQ potentiates the BAY-58-2667-induced decreases in TM cell volume. Data are expressed as % of initial volume at 0 time point and for: BAY-58-2667 (10 μM) treated group represents the mean ± SEM, n=38 cells; 8-Br-cGMP (2 mM) treated group represents the mean ± SEM , n= 30 cells; BAY-58-2667 + ODQ (5 μM) treated group represents the mean ± SEM, n= 48 cells and BAY-58-2667 + ODQ (10 μM) treated group represents the mean ± SEM, n= 44 cells. *Significantly different from control at P<0.05; ANOVA and the Holm-Sidak method. #Significantly different from BAY-58-2667 (10 μM) treated group at P<0.05; ANOVA and the Holm-Sidak method. D) BAY-58-2667-induced decrease in cell volume is associated with increases in cGMP. Levels of cGMP in TM cells after incubation with BAY-58-2667 (1-100 μM). Results measured are expressed as mean ± SEM fmol of cGMP done in quadruplicate.

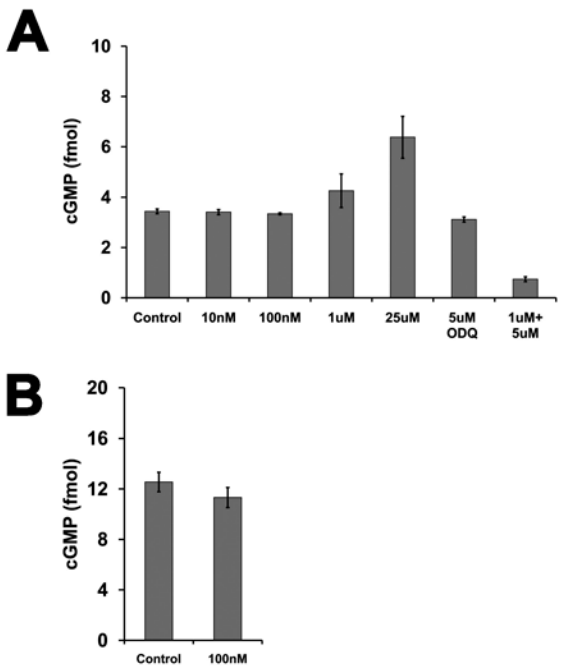

Figure 4-3. Low concentration YC-1 and BAY-58-2667 -induced increases in cell volume are not associated with significant increases in cGMP. A) Levels of cGMP in TM cells after incubation with YC-1 (10 nM – 25 μM) and YC-1 (1 μM) plus ODQ (5 μM). Results measured are expressed as mean ± SEM fmol of cGMP done in triplicate. B) Levels of cGMP in TM cells after incubation with BAY-58-2667 (100 nM). Results measured are expressed as mean ± SEM fmol of cGMP done in quadruplicate.

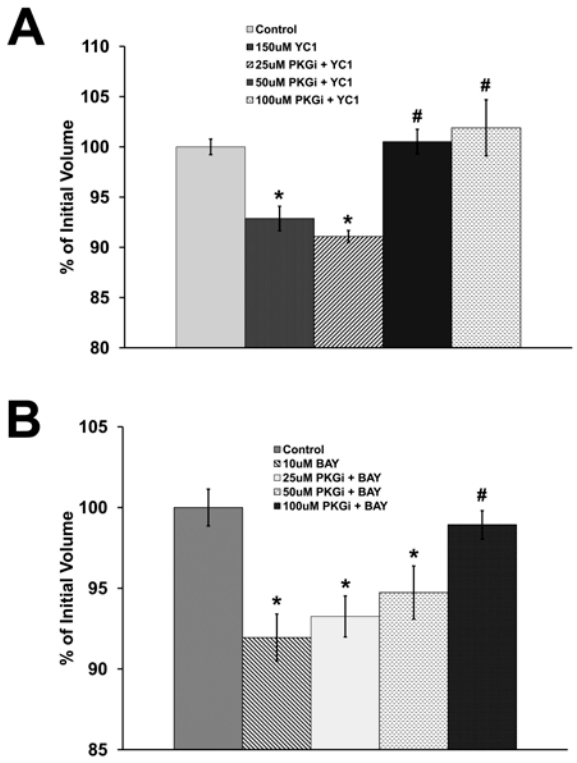

Figure 4-4. PKG is involved in the YC-1 and BAY-58-2667-induced decreases in TM cell volume. A) Cells were incubated with YC-1 (150 μM) in the presence or absence of varying concentrations of (RP)-8-Br-PET-cGMP-S, a PKG inhibitor (PKGi) (25 - 100 μM). Images were taken, and the cell volume was measured. Data are expressed as % of the initial volume at the 0-min time point and are means ± SEM; n =22 cells for the YC1 -treated group, n=21 cells for the YC-1 + PKGi (25 μM) -treated group, n =14 cells for the YC-1 + PKGi (50 μM) -treated group, and n=14 cells for the YC-1 + PKGi (100 μM) -treated group. *Significantly different from Control $p<0.05$ by ANOVA and the Holm-Sidak method; #significantly different from the 150 μM YC-1 treated group ($P < 0.05$) by ANOVA and the Holm-Sidak method. B) Cells were incubated with BAY-58-2667 (10 μM) in the presence or absence of varying concentrations of PKGi (25 - 100 μM). Images were taken, and the cell volume was measured. Data are expressed as % of the initial volume at the 0-min time point and are the means ± SEM; n =37 cells for the BAY-58-2667 -treated group, n=31 cells for the BAY-58-2667 + PKGi (25 μM) -treated group, n =84 cells for the BAY-58-2667 + PKGi (50 μM) -treated group, and n=25 cells for the BAY-58-2667 + PKGi (100 μM) -treated group. *Significantly different from Control $p<0.05$; #significantly different from the 10 μM BAY-58-2667 treated group ($P < 0.05$) by ANOVA and the Holm-Sidak method.

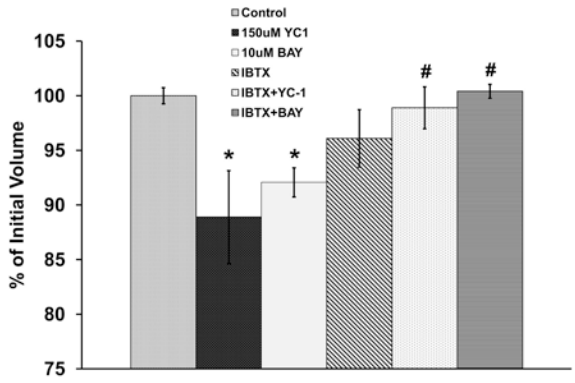

Figure 4-5. The YC-1 and BAY-58-2667 –induced decreases in TM cell volume involve the BK_{Ca} channel. TM cells were incubated with YC-1 (150 μM) and BAY-58-2667 (10 μM) in the presence or absence of IBTX (100 nM). Data are expressed as % of initial volume at 0 time point and represents the mean ± SEM; n =27 cells for the control group, n =23 cells for the YC1 -treated group, n= 37 cells for the BAY-58-2667 –treated group, n =19 cells for the IBTX -treated group, n =41 cells for the IBTX+YC1 -treated group and n=69 cells for the IBTX+BAY-58-2667-treated group. *Significantly different from the Control group and #significantly different from the YC-1 or BAY-58-2667- treated group ($P < 0.05$) ANOVA and the Fisher LSD method.

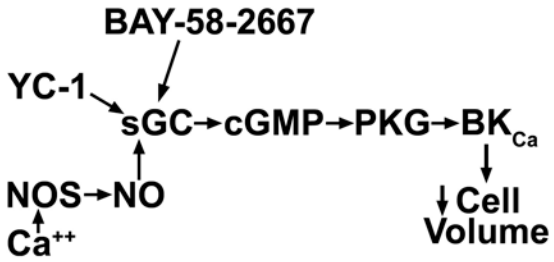

Figure 4-6. Summary diagram of the pathway of NO-dependent and NO-independent regulation of TM cell volume. Increases in $[Ca^{2+}]i$ result in activation of nitric oxide synthase (NOS), and the subsequent formation of NO, which then binds to and activates soluble guanylate cyclase (sGC). YC-1 and BAY-58-2667, NO-independent activators of sGC also bind to sGC and cause increases in cGMP. cGMP then activates PKG which may, directly or indirectly through other proteins, phosphorylate the BK_{Ca} channels, with subsequent K^+ efflux and decreases in cell volume.

CHAPTER 5
ACTIVATION OF THE BK_{CA} CHANNEL INCREASES OUTFLOW FACILITY AND DECREASES TRABECULAR MESHWORK CELL VOLUME

Introduction

Aqueous humor is secreted by the ciliary processes and exits the eye via the conventional pathway, consisting of the trabecular meshwork (TM) and Schlemm's canal. Increased resistance to outflow of aqueous humor in the TM and/or the Schlemm's canal results in increased intraocular pressure (IOP); a major risk factor for the development of open-angle glaucoma [37] . Viable treatment known to reduce the development and progression of blindness caused by glaucoma is decreasing IOP.

The mechanism(s) by which TM cells influence aqueous humor outflow is still not completely understood. It is postulated that TM cells may influence the tissue permeability, as agents that cause changes in cell volume [5, 7] , contractile states [44, 98] and cell shape [52] also modulate outflow facility.

The large conductance calcium-activated potassium channel (BK_{Ca}) consists of a tetramer of pore-forming α subunits associated with the regulatory β subunits in a 1:1 stoichiometry that when open allows for potassium efflux from the cell. The BK_{ca} channel has been shown to be activated by changes in membrane potential and intracellular calcium concentration [27] , cGMP-dependent protein phosphorylation events [28, 29] and by activators, including the benzimidazolone derivative, NS1619 [31] . Conversely, the channel is inhibited by charybdotoxin [99] and iberiotoxin (IBTX) [30] .

The BK_{Ca} channel has been shown to be involved in TM cell volume regulation and contractility. Specifically, it mediates the recovery of a hypotonic-induced decrease in outflow facility [5] suggesting its role in the TM cells regulatory volume decrease. The BKca channel also regulates the NO/cGMP-induced decreases in TM cell volume and increases in aqueous humor

outflow facility [90] . Additionally, cGMP increases the charybdotoxin-sensitive outward currents in bovine TM cells [45] suggesting the involvement of the BKca channel in the cGMP mediated relaxation of isolated bovine TM strips [26] . These events may not be mutually exclusive as both the cellular contractile mechanisms and the cell volume regulatory mechanisms may be functionally linked [50-52] .

In these studies we determined if direct activation of BK_{Ca} channel increases outflow facility. Additionally, we also tested the hypothesis that activation of the BK_{Ca} channels decrease TM cell volume in a time course that corresponds with the time course for activated BK_{Ca} channel-induced increase in outflow facility.

Materials and Methods

Cell Culture

Eyes from human donors with no history of ocular disease or surgery were obtained from Lions Eye Institute (Tampa, FL) within 24-30 hours postmortem. Primary human TM cell lines (numbers representing ages of the donors) (HTM26, HTM71, HTM36, HTM80 and HTM86) were developed as previously described [90] . For our experimental protocols cells from early passages (3-5) were used. TM cells were isolated after collagenase digestion of TM explants [64] . Collagenase-treated cells were grown in low glucose (1g/L) DMEM (Mediatech, Herdon VA.) in the presence of 10% fetal bovine serum (Mediatech, Herdon VA.), 100 U/ml penicillin and 100 μg/ml streptomycin (Mediatech, Herdon VA.). Cells were grown in 6-well culture dishes (Nalge Nunc International, Rochester, NY) in a tissue culture incubator @ $37^{o}C$ in 5% CO_2. Confluent cells were trypsinized and passaged. Prior to drug treatment, cells were transferred to a FluoroDish (World Precision Instruments, Inc) in low-glucose DMEM as described above after which they were exposed to serum free media for 2 days prior to performing the experiments.

Measurement of Cell Volume

Cell volume measurements were performed as previously described [90] . Prior to any drug treatments, the cells were loaded with the fluorescent dye Calcein AM in DMEM (~309 mOsm/kg) at 37°C, in 5% CO_2 incubator for 60 minutes to ensure a stable baseline. For changes in osmolarity, hypotonic media was made by addition of 30% deionized water to DMEM (~208 mOsm/kg). The coverslips containing the cells were subjected to confocal microscopy using a Leica confocal microscope. Changes in cell volume were determined by dividing the voxel count with drug treatment by the voxel count without drug treatment.

Outflow Facility Measurements

Outflow facility was measured using the anterior segment perfusion organ culture [67, 68] . Porcine eyes were obtained from the local abattoir within 1 hour postmortem and maintained on ice. Because morphological and biochemical studies suggested that the porcine anterior chamber perfusion model can be correlated with the human perfusion system [63] , perfusion studies were performed using porcine eyes. Eyes were bisected at the equator and the iris, lens and ciliary processes were removed. The anterior segments were cultured at 37°C in 100% humidity at 5% CO_2 atmosphere and perfused at constant pressure of 14 mmHg [69, 70] . The outflow rates were determined gravimetrically as the changes in weight of the media as the eyes were perfused over time and outflow facility was expressed as μl/min/mmHg perfusion pressure. Organ perfusions were performed with isotonic DMEM (~309 mOsm/kg) to establish baseline facility followed by perfusion with the drugs.

Materials and Reagents

Routine reagents, iberiotoxin (IBTX), and 1,3-Dihydro-1-[2-hydroxy-5-(trifluoromethyl)phenyl]-5-(trifluoromethyl)-2H-benzimidazol-2-one (NS1619) were purchased

from Sigma (St. Louis, MO). Diethylenetriamine NO (DETA-NO) from Sigma-RBI (Natick, MA).

Statistics

Statistical analysis was performed using ANOVA, followed by Holm-Sidak and Fisher LSD method for comparison of significant difference among different means.

Results

NS1619 Increases Outflow Facility

Outflow facility was measured in porcine anterior eye segments as described. Prior to drug treatment, eye anterior segments adapted to their new environment during which time outflow facility increased for several hours, a phenomenon referred to as "wash-out" [70, 71] after which outflow facility remained stable [63]. Basal outflow facility was 0.3815-0.4745 μl/min/mmHg among experiments and was stable for several hours prior to drug treatment and remained stable post drug effect. Because of the stability of the outflow facility baseline after the initial "wash-out" period, it was not necessary to correct for non-drug related changes in outflow facility in our experimental protocol.

Previous studies have demonstrated that NS1619 dose-dependently activated the outward current in aortic smooth muscle cells (3-30 μM) [31], relaxes precontracted rat basilar artery rings (EC_{50}=12.45+2.0 μM) [100] and partially attenuated a hypotonic-induced decrease in outflow facility in perfused bovine anterior segments (30 μM) [5]. To test the effect of NS1619 on outflow facility, NS1619 (30 μM) was added to the perfusate. This resulted in a significant increase in outflow facility, Figure 5-1. Outflow facility was increased immediately following drug treatment and reached statistical significance after 40 minutes. Outflow facility reached its maximal level, 0.7816+0.0528 μl/min/mmHg, at 80 minutes following application of the

NS1619 and the maximal effect of the drug was sustained for 3 hours after which outflow facility returned to values similar to baseline outflow facility. Values are representative of three separate experiments.

NS1619-induced Decrease in TM Cell Volume is Concentration-Dependent

Quantitative measurements of changes in cells volume in response to NS1619 were made in low passage human TM cells. Cells were exposed to varying concentrations of the drug (300 nM – 30 μM). Images were taken without drug treatment (0) time point, drugs were then added to the cells and images were taken of the same cells at 20 min as described. Using this protocol, each cell serves as its own control. Cells treated with vehicle only are also imaged at 20 min to ensure that the effects observed are as a result of changes in cell volume in response to drug treatment and not because of photo bleaching or the vehicle. Figure 5-2 demonstrates that there is a concentration-dependent decrease in TM cell volume in response to NS1619. While 300 nM NS1619 caused only a 3% decrease in cell volume, this decrease was significant when compared with the same cells before drug treatment. Addition of 3 μM and 30 μM NS1619 also resulted in significant decreases in cell volume, when compared with the same cells before drug treatment (7 and 10% changes respectively).

The BK_{Ca} Channel is Involved in TM Cell Regulatory Volume Decrease

To test that the effects of the BKCa channel on TM cell volume are not artifactual, cells were exposed to hypotonic media in the presence or absence of NS1619. Hypotonic media was made by addition of deionized water to DMEM for a final concentration of 30% water and 70% DMEM (~208 mOsm/kg). Images were captured of cells in isotonic media, after which the media were exchanged with hypotonic media and images were captured of the same cells at 1, 2, 3, 4 and 5 min. Figure 5-3 demonstrates that exposure of cells to hypotonic media resulted in a

7% increase in cell volume within 1 minute following application of hypotonic media after which cell volume returned to baseline without removal of the media. Cells exposed to NS1619 in the presence of hypotonic media resulted in a slight 1% increase in cell volume within 1 minute of changes in media conditions. One minute after the peak increase in cell volume, the cells experienced a significant decrease in cell volume after which cell volume returned to baseline conditions.

Effects of NS1619 and DETA-NO on Cell Volume Are Not Additive

We had previously demonstrated that the BKCa channel mediates the NO-induced increases in outflow facility and the NO-induced decreases in TM cell volume. Therefore in these studies we wanted to determine if the effects of NO on cell volume were additive in the presence of NS1619. TM cells were incubated with NS1619 only, with DETA-NO only, or with NS1619 in the presence of DETA-NO. Images were captured of the cells before drug treatment, after which the drugs were added and images captured at 20 minutes. There was a significant decrease in cell volume in response to both NS1619 and DETA-NO treatment. When both NS1619 and DETA-NO were added, cell volume decreases were equivalent to cell volume changes with either NS1619 or DETA-NO alone (Figure 5-4). To determine that the effects of NS1619 are occurring through activation of the BKca channel, TM cells were incubated with NS1619 in the presence of IBTX [30] . The NS1619-induced decrease in TM cell volume was abolished by preincubation with IBTX (Figure 5-4).

Discussion

To elucidate the role BKca channel activity plays in outflow facility and trabecular meshwork cell function, we utilized a direct activator of the BKca channel, NS1619. In these studies we demonstrate the ability of NS1619 to increase outflow facility in a time course that correlates with the NS1619-induced decreases in TM cell volume. Additionally, the decreases in

TM cell volume in response to NS1619 were equivalent to the decreases in cell volume observed in response to DETA-NO only, but in combination, NS1619 and DETA-NO produced no additive cell volume decrease.

Previous studies demonstrated the specificity of NS1619 to the BKca channel; exposure of bovine aortic smooth muscle cells [31] and rat cerebral arterial smooth muscle cells [100] to NS1619 resulted in increased open probability and outward currents that were blocked by the potassium channel blockers tetraethylammonium and charybdotoxin [31] or IBTX [100] suggesting the outward current and subsequent hyperpolarization of these cells are due to BKca channel activation. Additionally, NS1619 dose-dependently relaxed human coronary arterioles which was blocked by IBTX [101] . Furthermore, NS1619 selectively activates BKca channels and has been shown to have no effect on calcium, sodium, ATP-sensitive potassium or voltage gated potassium channels [31 ;27] .

The selectivity of NS1619 for activation of the BKca channel allowed us to determine the role BKca channel activity plays in determining outflow facility. The ability of NS1619 to increase outflow facility in porcine anterior segment provides new insight into the role of the BK_{Ca} channel in aqueous humor outflow. The NS1619-induced increases in outflow facility were immediate and transient and were sustained for 3 hours following bolus application of the drug after which outflow facility returned to baseline. These experiments are the first, to our knowledge, to demonstrate that BK_{Ca} channel opening regulates aqueous humor outflow. Other studies demonstrated that DETA-NO increased aqueous humor outflow facility, and this increase was abolished by the BK_{Ca} channel inhibitor, IBTX [90] , suggesting endogenous physiological regulation of the BK_{Ca} channel by the NO system.

To better understand the cellular mechanism by which BKca channel activity affects outflow facility, we examined the ability of NS1619 to cause changes in TM cell volume, a mechanism by which TM cells are thought to influence outflow [7 ;47 ;48 ;6 ;5 ;49] . Exposure of TM cells to NS1619 in isotonic media dose-dependently decreased cell volume in a time course that correlates with the NS1619-induced increases in outflow facility. While we did not determine the mechanism underlying the NS1619-induced cell volume decrease, electrophysiological studies in bovine aortic smooth muscle cells have demonstrated a NS1619-induced, dose-dependent leftward shift in the current-voltage relationship with the drug suggesting increased potassium efflux with increasing drug concentration [31] .

To further demonstrate the ability of the BKca channel to affect changes in TM cell volume, we included NS1619 in a hypotonic challenge and examined the drugs effect on regulatory volume decrease. NS1619 reduced the hypotonic-induced increase in TM cell volume. Previously, we demonstrated that inhibition of the BKca channel with IBTX potentiated the hypotonic-induced increases in cell volume and delayed the recovery to resting cell volume [90] . Similar results were demonstrated in another study; NS1619 when included in a hypotonic challenge to a perfused bovine eye reduced the decrease in outflow facility and quickened recovery to baseline. Conversely, IBTX potentiated the hypotonic-induced decreases in outflow facility and delayed recovery to baseline [5] . Taken together, these data provide further evidence that BKca channel activity modulates TM cell volume and this modulation of TM cell volume may affect outflow facility.

Incubation of TM cells with DETA-NO only, NS1619 only or DETA-NO in the presence of NS1619 resulted in decreased cell volume of similar magnitude suggesting that DETA-NO and NS1619 are not additive in decreasing cell volume. Released NO from DETA-NO is thought

to activate the BK_{Ca} channel via protein phosphorylation through protein kinase G [28, 29] . This PKG-dependent phosphorylation of the BKca channel increased the outward currents in rabbit arterial smooth muscle cells by increasing the voltage-dependent open probability of the channel [28] . A similar mechanism is suggested to underlie the actions of NS1619 on BKca channel activity [31, 100] . DETA-NO and NS1619 individually caused similar decreases in TM cell volume, but together showed no additive effect on cell volume, suggesting that activating the BKca channel with either DETA-NO or NS1619, presumably by altering the open probability of the channel, is sufficient to elicit a reduction in cell volume.

Additionally, previous studies showed that IBTX attenuated the NO-induced decreases in TM cell volume, suggesting that the BKca channel is involved in the cell volume decrease [90] . Similar results were demonstrated in these studies, as IBTX abolished the NS1619-induced decrease in TM cell volume. This provides another line of evidence suggesting the NS1619-induced reductions in TM cell volume are due to BKca channel activity. These reductions in TM cell volume with NS1619 in our experiments may be due to potassium efflux, as studies in the TM have demonstrated that inhibition of the BKca channel with IBTX is associated with inhibition of potassium conductance [102] . Potassium efflux through the BKca channel with possible parallel chloride efflux would tend to drive water out of the cytosol thus decreasing cell volume [95] .

We are mindful that there may not be a direct linkage between NS1619-induced changes in TM cell volume and outflow facility as in these studies we have not accounted for the possible involvement of the BKca channel in TM contractile mechanisms [45, 52] .

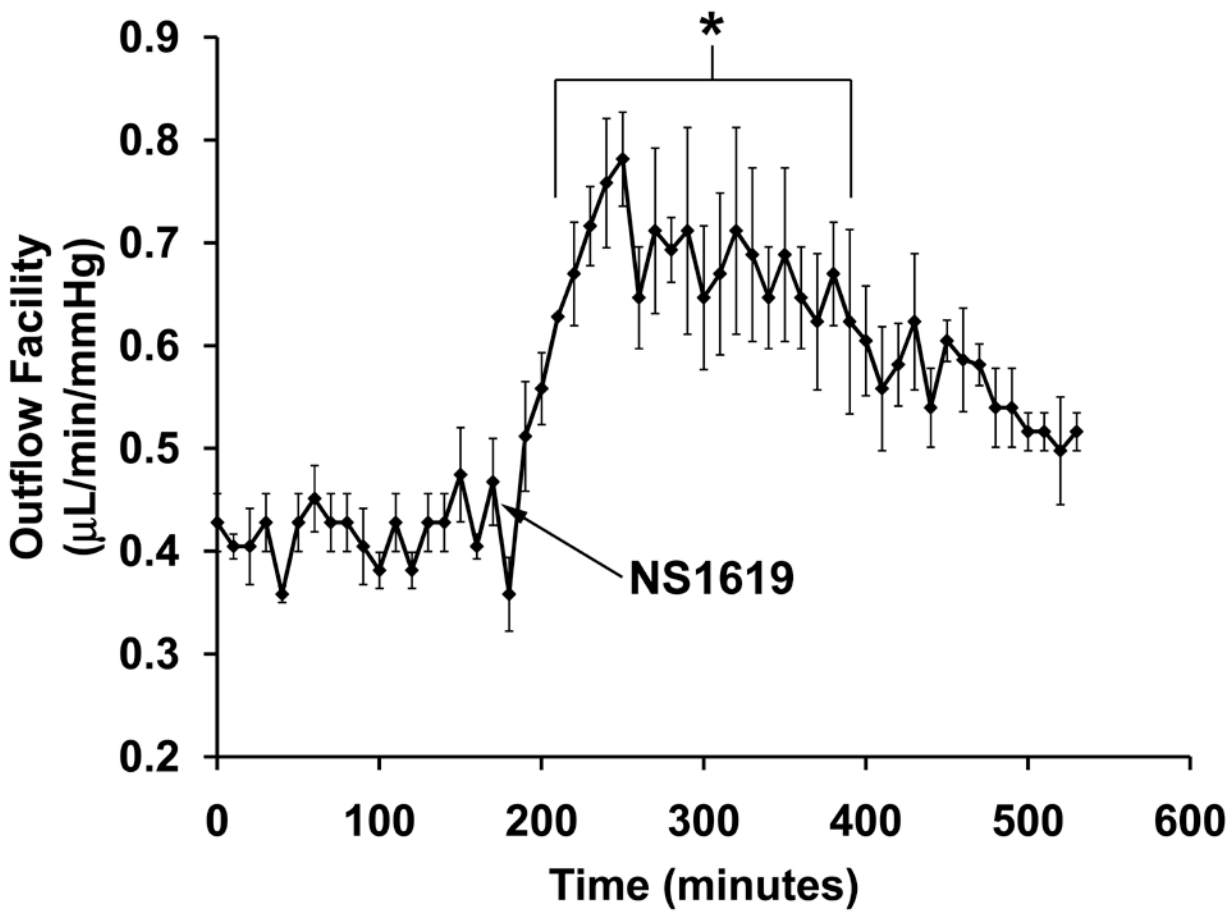

Figure 5-1. NS1619 increases outflow facility. A stable baseline was achieved after which the anterior chamber perfusate was replaced with an acute treatment of NS1619 (30μM) dissolved in ethanol (0.1 %, final concentration). Data shown is mean ± SEM for 3 experiments. *Significantly different from baseline values, $P<0.05$; ANOVA and the Fisher LSD method.

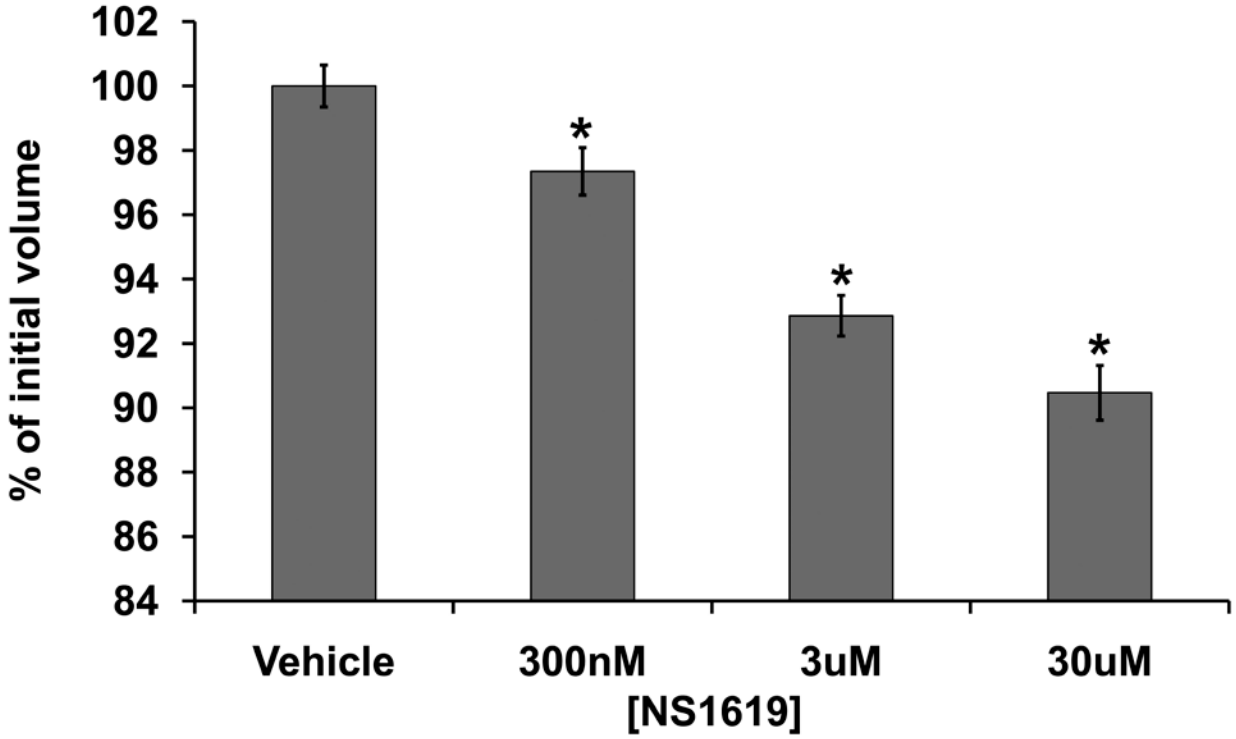

Figure 5-2. NS1619-induced decreases in TM cell volume are concentration dependent. Data are expressed as % of initial volume at 0 time point and for NS1619: 300 nM, mean ± SEM, n= 42 cells; 3 μM, mean ± SEM, n= 28 cells; and 30 μM, mean ± SEM, n= 34 cells *Significantly different from control at $P<0.05$; ANOVA and the Holm-Sidak method.

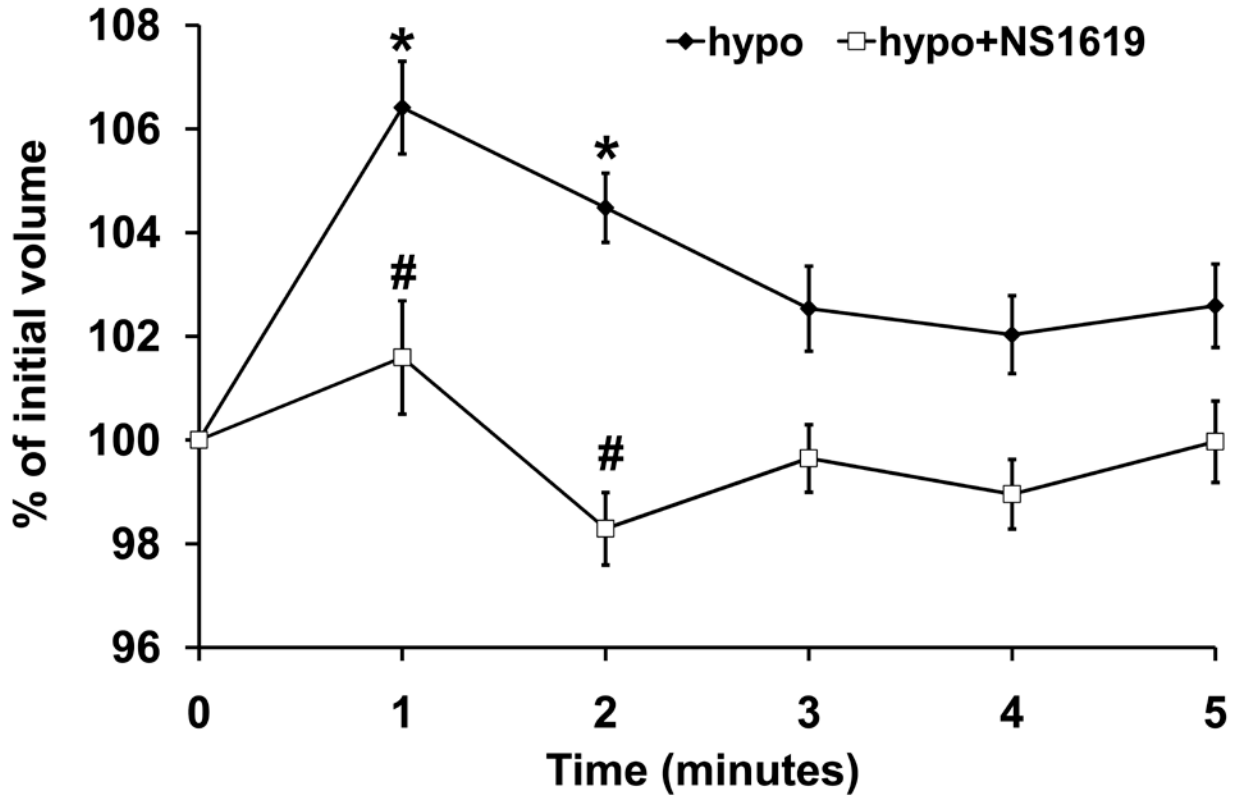

Figure 5-3. NS1619 abolishes the hypotonic-induced increases in TM cell volume. Hypotonic DMEM increased cell volume (mean ± SEM; n=36 cells). Cells were exposed to hypotonic medium in the presence of NS1619 (30 μM) and images were captured (mean ± SEM; n=35 cells). Data are expressed as % volume at 0 time point (isotonic medium). *Significantly different from 0 time point, $P<0.05$ and # significantly different from hypotonic treatment at 1 and 2 minutes, $P<0.05$ by ANOVA and the Holm-Sidak method.

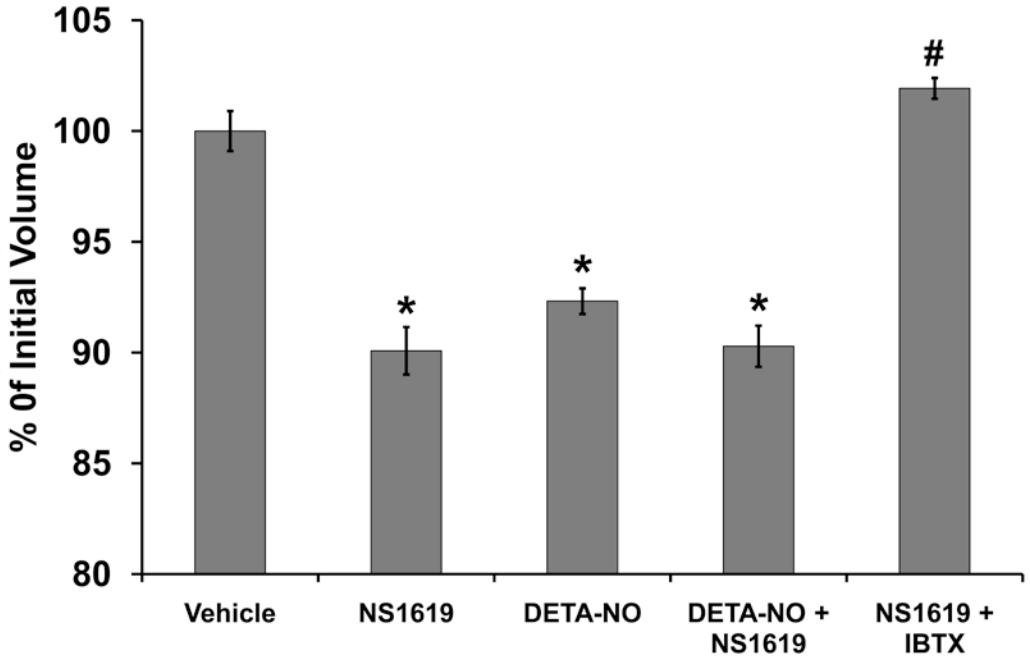

Figure 5-4. Actions of NS1619 and DETA-NO on TM cell volume are not additive and are abolished by IBTX. Cells were incubated with NS1619 (30 µM) alone, with DETA-NO (100 µM) alone, with NS1619 (30 µM) and DETA-NO (100 µM) or with NS1619 (30 µM) and IBTX (100 nM). Images were taken, and the cell volume was measured. Data are expressed as % of the initial volume at the 0-min time point and are means ± SEM; n= 24 cells for the NS1619 -treated group, n=28 cells for the DETA-NO treated group, n=13 cells for the NS1619 + DETA-NO -treated group, n=17 cells for the NS1619 + IBTX treated group. *Significantly different from vehicle $p<0.05$; by ANOVA and the Holm-Sidak method. #Significantly different from NS1619 $p<0.05$; by ANOVA and the Holm-Sidak method.

CHAPTER 6
CONCLUSION

Activation of Soluble Guanylate Cyclase and IOP

In this study we demonstrated;

1. The signal transduction pathway mediating the NO-induced increases in outflow facility and decreases in TM cell volume (figure 6-1).
2. The ability of the NO-independent sGC activators YC-1 and BAY-58-2667 to cause decreases in TM cell volume and increases in cGMP, involving activation sGC, PKG and the BKca channel.
3. Direct activation of the BKca channel mimics NO in increasing outflow facility and decreasing TM cell volume.

These provide the mechanism by which soluble guanylate cyclase activators regulate IOP in humans, rabbit and monkey [35, 59, 61, 62, 103-111] .

Studies have demonstrated that topical application of the NO donors to rabbit eyes [59] reduced IOP by increasing the rate of AH outflow through the TM [61] . Studies have also shown that intravitreal and intracameral injections of NO donors in rabbits caused a drastic decrease in IOP, which was correlated with nitrite production indicating that NO was released [62] . Additionally it has been shown that NO donors reduce IOP in monkeys through an action on outflow resistance [35] . While these actions on IOP are attributable to NO activating sGC, it is important to note that activators of both membrane guanylate cyclase[112, 112] and sGC have the ability to lower IOP. However, due to the pharmacokinetics of the peptide activators of membrane guanylate cyclase, they must be intravitreally applied to have an effect. This makes the IOP lowering effects mediated through sGC noteworthy, because many sGC activators can be topically applied to the eye to achieve an effect.

Although the IOP lowering ability of NO donors are known, little was known about the specific signal transduction pathway and cellular mechanism mediating the NO-induced increase

in outflow facility. Using perfused eye anterior segments, we found that the NO donor DETA-NO increased outflow facility within twenty minutes of the drugs application. Based on the literature, this rapid time course for outflow facility changes eliminated two cellular mechanisms thought to contribute to outflow regulation, alteration of the TM cytoskeleton and changes in the extracellular matrix of the TM. Both of these cellular mechanisms have been shown to affect outflow too slowly to account for our findings with DETA-NO. The other identified cellular mechanisms by which TM cells affect outflow facility, changes in cell volume and tissue contractility, do fit with our rapid changes in outflow facility with NO. We decided to examine the effect of DETA-NO on TM cell volume *in vitro*, using low passage TM cells and a confocal microscope. We measured the volume of TM cells over twenty minutes in five minute intervals and found DETA-NO dose-dependently lowered TM cell volume. To further ensure that the magnitude of cell volume change we were seeing with NO was appropriate to elicit a change in outflow facility, we treated perfused anterior segments with a hypertonic medium and measured the affect on outflow. Similarly, we treated our cultured cell with the same medium and measured cell volume. The results were consistent with our DETA-NO studies, reduced TM cell volume correlates with increases in outflow facility.

Using pharmalogical tools, we examined the signal transduction pathway mediating these cell volume decreases. By inhibiting sGC, protein kinase G or the BKca channel we blocked the ability of DETA-NO to cause TM cell volume decreases. Conversely, the cGMP analog 8-Br-cGMP mimicked the effects of DETA-NO on TM cell volume. With this knowledge in hand, we used the anterior segment perfusion system to demonstrate the requirement for BKca channel activity in the NO-induced increases in outflow facility.

With all of the evidence that NO acting on the TM lowers resistance to fluid flow, thus lowering IOP it was surprising that sGC in the TM had not been very well characterized. Without knowing the sGC isoforms and the relative abundance of sGC in the TM we have no ground to look at potential alterations in the enzyme that may have implications in the pathophysiology of open angle glaucoma. Prior to our studies of NO-independent sGC activators, we began to characterize sGC in cultured TM cells. In the low passage cell lines we tested, we found consistent expression of the α1 and β1 sGC isoforms in an equivalent ratio. The ratio of α to β subunit expression is important as the functional enzyme consist of an αβ heterodimer[113] . In these cells, DETA-NO treatment resulted in significant increases in cGMP. Interestingly, we could not detect a significant DETA-NO induced increase in cGMP in transformed human TM cells and demonstrated the these cells do not express the α and β sGC subunits in equal abundance[114] .

Still, further characterization of sGC in both the physiological and pathophysiological state is needed. It has been suggested that a subpopulation of patients with systemic hypertension have compromised NO-sGC signaling due to oxidation of or decreased abundance of the heme-moiety in sGC, a state rendering the enzyme incapable of being activated by NO[115] . Logically, a similar situation regarding the state of the sGC heme in the cells of the aqueous humor outflow pathway is possible, but yet unproven. Additionally, there are reports of reduced NOS abundance in the outflow pathway of patients with glaucoma[22] . In either of the cases, the ability to activate sGC in the TM would be diminished.

A patient with a reduced ability to activate sGC in TM cells may experience reduced aqueous humor outflow and increased IOP. Logically, adding exogenous NO to the anterior chamber may overcome the lack of endogenous NO production or activate the remaining,

undamaged sGC's, but may also have unintended, detrimental consequences detailed in chapter 1. Additionally, tolerance to the NO donor may develop, eliminating its ocular hypotensive properties[59] . Therefore we examined the effects of NO-independent activators of sGC.

YC-1 and BAY-58-2667

YC-1

In our studies we demonstrate the ability of YC-1, the first reported NO-independent activator of sGC[18] , to increase cGMP concentration and decrease TM cell volume in a manner dependent on activation of sGC, PKG and the BKca channel. Our data and data from the literature on YC-1 suggest YC-1 –like compounds may offer interesting properties as ocular hypotensive drugs. For example, YC-1 alone can stimulate sGC activity but, NO and YC-1 stimulate sGC activity synergistically. Similar to NO, YC-1 cannot activate a heme-independent or oxidized-heme sGC. Based on the similarities between YC-1 and NO in activating sGC, work with YC-1 has led to a better understanding of how NO activates sGC[116] . While we are interested in examining sGC activation in TM cells, our study of YC-1 on the cells of the outflow pathway is not without precedent. Topically applied YC-1 has been shown to reduce IOP in normotensive rabbits[19] .

Since the discovery of YC-1's potential to activate sGC, a number of other compounds have been synthesized which show sGC stimulating properties. These compounds fall into two groups, heme-dependent and heme-independent sGC activators. As stated above, YC-1 is a heme-dependent sGC activator and cannot activate sGC if the heme moiety is oxidized or absent. In our study of NO-independent sGC activators, in addition to YC-1, we selected a heme-independent sGC activator BAY-58-2667 and examined its effects on TM cell volume.

BAY-58-2667

In our studies we demonstrate the ability of BAY-58-2667 to increase cGMP concentration, and dose-dependently reduce TM cell volume through activation of PKG and the BKca channel. Unlike YC-1, cells treated with ODQ experienced a potentiation of the BAY-58-2667 induced cell volume decrease. BAY-58-2667 was first described in 2002[93] . In this study, the investigators demonstrate the sGC activating properties of BAY-58-2667 alone. This sGC activation was addititive with BAY-58-2667 and a NO donor. Interestingly, when the sGC inhibitor ODQ was added with the BAY-58-2667 there was a potentiation of the BAY-58-2667 induced stimulation of sGC activity as opposed to the sGC inhibition seen with NO or YC-1 in the presence of ODQ. Additionally, BAY-58-2667 could stimulate heme-free sGC activity unlike NO or YC-1. These heme-independent sGC activating properties made BAY-58-2667 an interesting compound to include in our study.

The results we obtained with both YC-1 and BAY-58-2667 fit well with studies on these compounds outside the eye. Both dose-dependently reduced TM cell volume, although BAY-58-2667 appeared to be more effacious and potent. Both increase cGMP levels in cultured TM cells. They both appeared to activate the same signal transduction pathway as inhibitors of PKG and the BKca channel attenuated their effects on TM cell volume. In line with the literature, we could inhibit the YC-1 induced cell volume decrease with ODQ, while ODQ potentiated the cell volume reduction seen with BAY-58-2667 alone.

Based on our findings and those in the literature, we can conclude that these NO-independent sGC activating compounds may have ocular hypotensive properties of clinical significance. The interesting implication is that heme-dependent sGC activators like YC-1 may benefit a patient with reduced endogenous NO production, but functional sGC. In this patient, the synergy of a YC-1-like compound with the reduced NO production may restore sGC activity

to normal levels. This has an advantage over simply adding exogenous NO to the eye, as there is a much lower potential for deleterious sGC-independent NO effects. The possibility also exist that an ocular hypertensive patient may have normal NOS activity in the outflow pathway, but a compromised sGC system, possibly due to oxidation of the heme moiety. In this patient, adding excess NO would have very little effect on increasing cGMP and decreasing IOP. However, the use of a NO-independent, heme-independent sGC activator like BAY-58-2667 could restore normal sGC-cGMP activity and lower IOP.

While YC-1 has been shown to lower IOP in normotensive rabbits, to date no one has demonstrated the ocular hypotensive effects of BAY-58-2667. More importantly, neither compound has been shown to lower IOP in an ocular hypertensive patient or animal model, a critical step in gaining traction to become a clinically beneficial ocular hypotensive treatment.

Direct Activation of the Large-Conductance, Calcium-Activated Potassium Channel

We demonstrated that in a perfused eye anterior segment that the well characterized, direct BKca channel activator NS1619 alone was capable of significantly increasing outflow facility. Similar to DETA-NO, NS1619 reduced TM cell volume in a dose-dependent manner. We also found that in combination, NS1619 and DETA-NO gave no additive reduction in TM cell volume when compared to either alone.

In chapter 3, we found that applying the BKca channel blocker IBTX following a NO-induced increase in outflow facility could immediately return outflow facility to baseline values, indicating sustained BKca channel activation is required for the NO-induced increase. Our results indicate activation of the BKca channel in TM cells is all that is required to initiate a reduction in cell volume or increase in outflow facility. This raises two interesting questions; do direct activators of the BKca channel have clinically significant ocular hypotensive properties and what role, if any, does the BKca channel have in the pathophysiology of open angle

glaucoma? While our findings indicate BKca channel activation increases outflow facility, our data does not account for actions on BKca channel stimulation in other tissue of the eye, which may interfere with our goal of lowering intraocular pressure. These concerns could be addressed with topically applied NS1619 in an animal model. We could then begin to understand the net effect of BKca channel stimulation in the eye. Secondly, it would be of interest to examine the functioning of the BKca channel in TM cells from a glaucomatous patient. The possibility exists that in some forms of ocular hypertension the BKca channel may be in reduced abundance or not responsive to the physiological means of activation.

Physiological Significance

The mechanism by which aqueous humor drainage from the eye and ultimately IOP is controlled is, to date, not fully understood. We have begun to dissect the cellular mechanisms mediating pharmacological changes in outflow facility, but much work must still be done. Our work in the TM has added to the understanding of how one endogenous modulator of outflow facility, NO, affects the TM cells. By identifying the signal transduction pathway mediating the NO-induced increases in outflow and decreases in TM cell volume, we were able to identify and characterize the role sGC and the BKca channel play in affecting outflow facility. Our work indicates that these two pharmacological targets hold promise for the development of novel ocular hypotensive strategies.

Future Directions

The studies presented here have only addressed the trabecular meshwork, one of the components associated with aqueous humor drainage. We have now begun to look at the effect of NO on the Schlemm's canal. The relationship between the Schlemm's canal, the TM and how they in combination control aqueous humor drainage is not well understood. The data obtained regarding NO and the cells of the Schlemm's canal may help unravel the contribution each

provides in resistance to aqueous drainage as well as how they work in combination. Additionally, our data are from *in vitro* studies and perfused porcine anterior eye segments. The next step towards determining the ocular hypotensive potential for compounds like BAY-58-2667 and NS1619 would involve topical application to the eye in a normotensive and ocular hypertensive animal model while monitoring IOP and outflow.

LIST OF REFERENCES

1. Lee WR, Grierson P, McMenamin PG. The Morphological Response of the Primate Outflow System. In: Lutjen-Drecoll E (ed), *Basic Aspects of Glaucoma Research* Stuttgart: F.K. Schattauer; 1982:123-139.

2. Kaufman PL. Aqueous humor outflow. *Curr Top Eye Res*. 1984;4:97-138.

3. Krupin T, Civan MM. The physiological basis of aqueous humor formation. In: Ritch R, Shields MB (eds), *The Glaucomas* St. Louis: Mosby; 1995:251-280.

4. Mitchell CH, Fleischhauer JC, Stamer WD, Peterson-Yantorno K, Civan MM. Human trabecular meshwork cell volume regulation. *Am J Physiol Cell Physiol*. 2002;283:C315-C326.

5. Soto D, Comes N, Ferrer E, et al. Modulation of aqueous humor outflow by ionic mechanisms involved in trabecular meshwork cell volume regulation. *Invest Ophthalmol Vis Sci*. 2004;45:3650-3661.

6. O'Donnell ME, Brandt JD, Curry FR. Na-K-Cl cotransport regulates intracellular volume and monolayer permeability of trabecular meshwork cells. *Am J Physiol*. 1995;268:C1067-C1074.

7. Al-Aswad LA, Gong H, Lee D, et al. Effects of Na-K-2Cl cotransport regulators on outflow facility in calf and human eyes in vitro. *Invest Ophthalmol Vis Sci*. 1999;40:1695-1701.

8. Stumpff F, Wiederholt M. Regulation of trabecular meshwork contractility. *Ophthalmologica*. 2000;214:33-53.

9. Bradley JM, Vranka J, Colvis CM, et al. Effect of matrix metalloproteinases activity on outflow in perfused human organ culture. *Invest Ophthalmol Vis Sci*. 1998;39:2649-2658.

10. Grierson I, Johnson NF. The post-mortem vacuoles of Schlemm's canal. *Albrecht Von Graefes Arch Klin Exp Ophthalmol*. 1981;215:249-264.

11. Polansky JR, Wood IS, Maglio MT, Alvarado JA. Trabecular meshwork cell culture in glaucoma research: evaluation of biological activity and structural properties of human trabecular cells in vitro. *Ophthalmology*. 1984;91:580-595.

12. Alexander JP, Samples JR, Van Buskirk EM, Acott TS. Expression of matrix metalloproteinases and inhibitor by human trabecular meshwork. *Invest Ophthalmol Vis Sci*. 1991;32:172-180.

13. Thomas DD, Liu X, Kantrow SP, Lancaster JR, Jr. The biological lifetime of nitric oxide: implications for the perivascular dynamics of NO and O2. *Proc Natl Acad Sci U S A*. 2001;98:355-360.

14. Murad F. Nitric oxide signaling: would you believe that a simple free radical could be a second messenger, autacoid, paracrine substance, neurotransmitter, and hormone? *Recent Prog Horm Res*. 1998;53:43-59.

15. Lucas KA, Pitari GM, Kazerounian S, et al. Guanylyl cyclases and signaling by cyclic GMP. *Pharmacol Rev*. 2000;52:375-414.

16. Ford PC, Wink DA, Stanbury DM. Autoxidation kinetics of aqueous nitric oxide. *FEBS Lett*. 1993;326:1-3.

17. Beckman JS, Koppenol WH. Nitric oxide, superoxide, and peroxynitrite: the good, the bad, and the ugly. *Am J Physiol*. 1996;271:C1424-C1437.

18. Ko FN, Wu CC, Kuo SC, Lee FY, Teng CM. YC-1, a novel activator of platelet guanylate cyclase. *Blood*. 1994;84:4226-4233.

19. Kotikoski H, Alajuuma P, Moilanen E, et al. Comparison of nitric oxide donors in lowering intraocular pressure in rabbits: role of cyclic GMP. *J Ocul Pharmacol Ther*. 2002;18:11-23.

20. Martin E, Lee YC, Murad F. YC-1 activation of human soluble guanylyl cyclase has both heme-dependent and heme-independent components. *Proc Natl Acad Sci U S A*. 2001;98:12938-12942.

21. Mulsch A, Bauersachs J, Schafer A, Stasch JP, Kast R, Busse R. Effect of YC-1, an NO-independent, superoxide-sensitive stimulator of soluble guanylyl cyclase, on smooth muscle responsiveness to nitrovasodilators. *Br J Pharmacol*. 1997;120:681-689.

22. Nathanson JA, McKee M. Alterations of ocular nitric oxide synthase in human glaucoma. *Invest Ophthalmol Vis Sci*. 1995;36:1774-1784.

23. Lamothe M, Chang FJ, Balashova N, Shirokov R, Beuve A. Functional characterization of nitric oxide and YC-1 activation of soluble guanylyl cyclase: structural implication for the YC-1 binding site? *Biochemistry*. 2004;43:3039-3048.

24. Stasch JP, Alonso-Alija C, Apeler H, et al. Pharmacological actions of a novel NO-independent guanylyl cyclase stimulator, BAY 41-8543: in vitro studies. *Br J Pharmacol*. 2002;135:333-343.

25. Stumpff F, Strauss O, Boxberger M, Wiederholt M. Characterization of maxi-K-channels in bovine trabecular meshwork and their activation by cyclic guanosine monophosphate. *Invest Ophthalmol Vis Sci*. 1997;38:1883-1892.

26. Wiederholt M, Sturm A, Lepple-Wienhues A. Relaxation of trabecular meshwork and ciliary muscle by release of nitric oxide. *Invest Ophthalmol Vis Sci*. 1994;35:2515-2520.

27. Ghatta S, Nimmagadda D, Xu X, O'Rourke ST. Large-conductance, calcium-activated potassium channels: structural and functional implications. *Pharmacol Ther*. 2006;110:103-116.

28. Robertson BE, Schubert R, Hescheler J, Nelson MT. cGMP-dependent protein kinase activates Ca-activated K channels in cerebral artery smooth muscle cells. *Am J Physiol*. 1993;265:C299-C303.

29. Alioua A, Tanaka Y, Wallner M, et al. The large conductance, voltage-dependent, and calcium-sensitive K+ channel, Hslo, is a target of cGMP-dependent protein kinase phosphorylation in vivo. *J Biol Chem*. 1998;273:32950-32956.

30. Galvez A, Gimenez-Gallego G, Reuben JP, et al. Purification and characterization of a unique, potent, peptidyl probe for the high conductance calcium-activated potassium channel from venom of the scorpion Buthus tamulus. *J Biol Chem*. 1990;265:11083-11090.

31. Olesen SP, Munch E, Moldt P, Drejer J. Selective activation of Ca(2+)-dependent K+ channels by novel benzimidazolone. *Eur J Pharmacol*. 1994;251:53-59.

32. Zhou L, Zhang SR, Yue BY. Adhesion of human trabecular meshwork cells to extracellular matrix proteins. Roles and distribution of integrin receptors. *Invest Ophthalmol Vis Sci*. 1996;37:104-113.

33. Stamer WD, Roberts BC, Howell DN, Epstein DL. Isolation, culture, and characterization of endothelial cells from Schlemm's canal. *Invest Ophthalmol Vis Sci*. 1998;39:1804-1812.

34. Kaufman PL, BARANY EH. Cytochalasin B reversibly increases outflow facility in the eye of the cynomolgus monkey. *Invest Ophthalmol Vis Sci*. 1977;16:47-53.

35. Schuman JS, Erickson K, Nathanson JA. Nitrovasodilator effects on intraocular pressure and outflow facility in monkeys. *Exp Eye Res*. 1994;58:99-105.

36. Mitchell CH, Fleischhauer JC, Stamer WD, Peterson-Yantorno K, Civan MM. Human trabecular meshwork cell volume regulation. *Am J Physiol*. 2002;283:C315-C326.

37. Lutjen-Drecoll E. Importance of trabecular meshwork changes in the pathogenesis of primary open-angle glaucoma. *J Glaucoma*. 2000;9:417-418.

38. Fuchshofer R, Welge-Lussen U, Lutjen-Drecoll E, Birke M. Biochemical and morphological analysis of basement membrane component expression in corneoscleral and cribriform human trabecular meshwork cells. *Invest Ophthalmol Vis Sci*. 2006;47:794-801.

39. Coroneo MT, Korbmacher C, Flugel C, Stiemer B, Lutjen-Drecoll E, Wiederholt M. Electrical and morphological evidence for heterogeneous populations of cultured bovine trabecular meshwork cells. *Exp Eye Res*. 1991;52:375-388.

40. Fleischhauer JC, Mitchell CH, Stamer WD, Karl MO, Peterson-Yantorno K, Civan MM. Common actions of adenosine receptor agonists in modulating human trabecular meshwork cell transport. *J Membr Biol*. 2003;193:121-136.

41. Barany EH. The mode of action of pilocarpine on outflow resistance in the eye of a primate (Cercopithecus ethiops). *Invest Ophthalmol*. 1962;1:712-727.

42. Lepple-Wienhues A, Stahl F, Wiederholt M. Differential smooth muscle-like contractile properties of trabecular meshwork and ciliary muscle. *Exp Eye Res*. 1991;53:33-38.

43. Wiederholt M. Direct involvement of trabecular meshwork in the regulation of aqueous humor outflow. *Curr Opin Ophthalmol*. 1998;9:46-49.

44. Llobet A, Gual A, Pales J, Barraquer R, Tobias E, Nicolas JM. Bradykinin decreases outflow facility in perfused anterior segments and induces shape changes in passaged BTM cells in vitro. *Invest Ophthalmol Vis Sci*. 1999;40:113-125.

45. Wiederholt M, Thieme H, Stumpff F. The regulation of trabecular meshwork and ciliary muscle contractility. *Prog Retin Eye Res*. 2000;19:271-295.

46. Rao PV, Deng PF, Kumar J, Epstein DL. Modulation of aqueous humor outflow facility by the Rho kinase-specific inhibitor Y-27632. *Invest Ophthalmol Vis Sci*. 2001;42:1029-1037.

47. Freddo TF, Patterson MM, Scott DR, Epstein DL. Influence of mercurial sulfhydryl agents on aqueous outflow pathways in enucleated eyes. *Invest Ophthalmol Vis Sci*. 1984;25:278-285.

48. Gual A, Llobet A, Gilabert R, et al. Effects of time of storage, albumin, and osmolality changes on outflow facility (C) of bovine anterior segment in vitro. *Invest Ophthalmol Vis Sci*. 1997;38:2165-2171.

49. Srinivas SP, Maertens C, Goon LH, et al. Cell volume response to hyposmotic shock and elevated cAMP in bovine trabecular meshwork cells. *Exp Eye Res*. 2004;78:15-26.

50. Ziyadeh FN, Mills JW, Kleinzeller A. Hypotonicity and cell volume regulation in shark rectal gland: role of organic osmolytes and F-actin. *Am J Physiol*. 1992;262:F468-F479.

51. Henson JH, Roesener CD, Gaetano CJ, et al. Confocal microscopic observation of cytoskeletal reorganizations in cultured shark rectal gland cells following treatment with hypotonic shock and high external K+. *J Exp Zool*. 1997;279:415-424.

52. Tian B, Geiger B, Epstein DL, Kaufman PL. Cytoskeletal involvement in the regulation of aqueous humor outflow. *Invest Ophthalmol Vis Sci*. 2000;41:619-623.

53. Benham CD, Bolton TB, Lang RJ, Takewaki T. Calcium-activated potassium channels in single smooth muscle cells of rabbit jejunum and guinea-pig mesenteric artery. *J Physiol*. 1986;371:45-67.

54. Nelson MT, Cheng H, Rubart M, et al. Relaxation of arterial smooth muscle by calcium sparks. *Science*. 1995;270:633-637.

55. Singer JJ, Walsh JV, Jr. Characterization of calcium-activated potassium channels in single smooth muscle cells using the patch-clamp technique. *Pflugers Arch*. 1987;408:98-111.

56. Sausbier M, Schubert R, Voigt V, et al. Mechanisms of NO/cGMP-dependent vasorelaxation. *Circ Res*. 2000;87:825-830.

57. Nathanson JA, McKee M. Identification of an extensive system of nitric oxide-producing cells in the ciliary muscle and outflow pathway of the human eye. *Invest Ophthalmol Vis Sci*. 1995;36:1765-1773.

58. Selbach JM, Gottanka J, Wittmann M, Lutjen-Drecoll E. Efferent and afferent innervation of primate trabecular meshwork and scleral spur. *Invest Ophthalmol Vis Sci*. 2000;41:2184-2191.

59. Nathanson JA. Nitrovasodilators as a new class of ocular hypotensive agents. *J Pharmacol Exp Ther*. 1992;260:956-965.

60. Giuffrida S, Bucolo C, Drago F. Topical application of a nitric oxide synthase inhibitor reduces intraocular pressure in rabbits with experimental glaucoma. *J Ocular Pharmacol Ther*. 2003;19:527-534.

61. Kotikoski H, Vapaatalo H, Oksala O. Nitric oxide and cyclic GMP enhance aqueous humor outflow facility in rabbits. *Curr Eye Res*. 2003;26:119-123.

62. Behar-Cohen FF, Goureau O, d'Hermies F, Courtois Y. Decreased intraocular pressure induced by nitric oxide donors is correlated to nitrite production in the rabbit eye. *Invest Ophthalmol Vis Sci*. 1996;37:1711-1715.

63. Bachmann B, Birke M, Kook D, Eichhorn M, Lutjen-Drecoll E. Ultrastructural and biochemical evaluation of the porcine anterior chamber perfusion model. *Invest Ophthalmol Vis Sci*. 2006;47:2011-2020.

64. Stamer WD, Seftor RE, Williams SK, Samaha HA, Snyder RW. Isolation and culture of human trabecular meshwork cells by extracellular matrix digestion. *Curr Eye Res*. 1995;14:611-617.

65. Bush PG, Hall AC. The volume and morphology of chondrocytes within non-degenerate and degenerate human articular cartilage. *Osteoarthritis Cartilage*. 2003;11:242-251.

66. Bush PG, Hodkinson PD, Hamilton GL, Hall AC. Viability and volume of in situ bovine articular chondrocytes-changes following a single impact and effects of medium osmolarity. *Osteoarthritis Cartilage*. 2005;13:54-65.

67. Johnson DH, Tschumper RC. Human trabecular meshwork organ culture. A new method. *Invest Ophthalmol Vis Sci*. 1987;28:945-953.

68. Johnson DH, Tschumper RC. The effect of organ culture on human trabecular meshwork. *Exp Eye Res*. 1989;49:113-127.

69. Erickson-Lamy K, Rohen JW, Grant WM. Outflow facility studies in the perfused bovine aqueous outflow pathways. *Curr Eye Res*. 1988;7:799-807.

70. Overby D, Gong H, Qiu G, Freddo TF, Johnson M. The mechanism of increasing outflow facility during washout in the bovine eye. *Invest Ophthalmol Vis Sci*. 2002;43:3455-3464.

71. Erickson-Lamy K, Schroeder AM, Bassett-Chu S, Epstein DL. Absence of time-dependent facility increase ("washout") in the perfused enucleated human eye. *Invest Ophthalmol Vis Sci*. 1990;31:2384-2388.

72. Clemo HF, Feher JJ, Baumgarten CM. Modulation of rabbit ventricular cell volume and Na+/K+/2Cl- cotransport by cGMP and atrial natriuretic factor. *J Gen Physiol*. 1992;100:89-114.

73. Garthwaite J, Southam E, Boulton CL, Nielsen EB, Schmidt K, Mayer B. Potent and selective inhibition of nitric oxide-sensitive guanylyl cyclase by 1H-[1,2,4]oxadiazolo[4,3-a]quinoxalin-1-one. *Molec Pharmacol*. 1995;48:184-188.

74. Ellis DZ, Nathanson JA, Sweadner KJ. Carbachol inhibits Na^+-K^+-ATPase activity in choroid plexus via stimulation of the NO/cGMP pathway. *Am J Physiol*. 2000;279:C1685-C1693.

75. Scavone C, Scanlon C, McKee M, Nathanson JA. Atrial natriuretic peptide modulates sodium and potassium-activated adenosine triphosphatase through a mechanism involving cyclic GMP and cyclic GMP-dependent protein kinase. *J Pharmacol Exp Ther*. 1995;272:1036-1043.

76. Butt E, Pohler D, Genieser HG, Huggins JP, Bucher B. Inhibition of cyclic GMP-dependent protein kinase-mediated effects by (Rp)-8-bromo-PET-cyclic GMPS. *Br J Pharmacol*. 1995;116:3110-3116.

77. Kee C, Kaufman PL, Gabelt BT. Effect of 8-Br cGMP on aqueous humor dynamics in monkeys. *Invest Ophthalmol Vis Sci*. 1994;35:2769-2773.

78. Tanaka Y, Koike K, Toro L. MaxiK channel roles in blood vessel relaxations induced by endothelium-derived relaxing factors and their molecular mechanisms. *J Smooth Muscle Res*. 2004;40:125-153.

79. Krupin T, Weiss A, Becker B, Holmberg N, Fritz C. Increased intraocular pressure following topical azide or nitroprusside. *Invest Ophthalmol Vis Sci*. 1977;16:1002-1007.

80. Feelisch M. The use of nitric oxide donors in pharmacological studies. *Naunyn Schmiedebergs Arch Pharmacol*. 1998;358:113-122.

81. Comes N, Abad E, Morales M, Borras T, Gual A, Gasull X. Identification and functional characterization of ClC-2 chloride channels in trabecular meshwork cells. *Exp Eye Res*. 2006;83:877-889.

82. Acott TS, Kingsley PD, Samples JR, Van Buskirk EM. Human trabecular meshwork organ culture: morphology and glycosaminoglycan synthesis. *Invest Ophthalmol Vis Sci*. 1988;29:90-100.

83. Clemo HF, Baumgarten CM, Ellenbogen KA, Stambler BS. Atrial natriuretic peptide and cardiac electrophysiology: autonomic and direct effects. *J Cardiovasc Electrophysiol*. 1996;7:149-162.

84. Putney LK, Brandt JD, O'Donnell ME. Na-K-Cl cotransport in normal and glaucomatous human trabecular meshwork cells. *Invest Ophthalmol Vis Sci*. 1999;40:425-434.

85. Larsen AK, Jensen BS, Hoffmann EK. Activation of protein kinase C during cell volume regulation in Ehrlich mouse ascites tumor cells. *Biochim Biophys Acta*. 1994;1222:477-482.

86. Gabelt BT, Wiederholt M, Clark AF, Kaufman PL. Anterior segment physiology after bumetanide inhibition of Na-K-Cl cotransport. *Invest Ophthalmol Vis Sci*. 1997;38:1700-1707.

87. Garbers DL. Purification of soluble guanylate cyclase from rat lung. *J Biol Chem*. 1979;254:240-243.

88. Wedel B, Harteneck C, Foerster J, Friebe A, Schultz G, Koesling D. Functional domains of soluble guanylyl cyclase. *J Biol Chem*. 1995;270:24871-24875.

89. Arnold WP, Mittal CK, Katsuki S, Murad F. Nitric oxide activates guanylate cyclase and increases guanosine 3':5'-cyclic monophosphate levels in various tissue preparations. *Proc Natl Acad Sci U S A*. 1977;74:3203-3207.

90. Dismuke WM, Mbadugha CC, Ellis DZ. NO-induced regulation of human trabecular meshwork cell volume and aqueous humor outflow facility involve the BKCa ion channel. *Am J Physiol Cell Physiol*. 2008;294:C1378-C1386.

91. Schmidt PM, Schramm M, Schroder H, Wunder F, Stasch JP. Identification of residues crucially involved in the binding of the heme moiety of soluble guanylate cyclase. *J Biol Chem*. 2004;279:3025-3032.

92. Wu CC, Ko FN, Kuo SC, Lee FY, Teng CM. YC-1 inhibited human platelet aggregation through NO-independent activation of soluble guanylate cyclase. *Br J Pharmacol*. 1995;116:1973-1978.

93. Stasch JP, Schmidt P, onso-Alija C, et al. NO- and haem-independent activation of soluble guanylyl cyclase: molecular basis and cardiovascular implications of a new pharmacological principle. *Br J Pharmacol*. 2002;136:773-783.

94. Schmidt P, Schramm M, Schroder H, Stasch JP. Mechanisms of nitric oxide independent activation of soluble guanylyl cyclase. *Eur J Pharmacol*. 2003;468:167-174.

95. Okada Y, Maeno E, Shimizu T, Dezaki K, Wang J, Morishima S. Receptor-mediated control of regulatory volume decrease (RVD) and apoptotic volume decrease (AVD). *J Physiol*. 2001;532:3-16.

96. Ellis DZ, Nathanson JA, Rabe J, Sweadner KJ. Carbachol and nitric oxide inhibition of Na,K-ATPase activity in bovine ciliary processes. *Invest Ophthalmol Vis Sci*. 2001;42:2625-2631.

97. Shahidullah M, Delamere NA. NO donors inhibit Na,K-ATPase activity by a protein kinase G-dependent mechanism in the nonpigmented ciliary epithelium of the porcine eye. *Br J Pharmacol*. 2006;148:871-880.

98. Krauss AH, Wiederholt M, Sturm A, Woodward DF. Prostaglandin effects on the contractility of bovine trabecular meshwork and ciliary muscle. *Exp Eye Res*. 1997;64:447-453.

99. Miller C, Moczydlowski E, Latorre R, Phillips M. Charybdotoxin, a protein inhibitor of single Ca2+-activated K+ channels from mammalian skeletal muscle. *Nature*. 1985;313:316-318.

100. Holland M, Langton PD, Standen NB, Boyle JP. Effects of the BKCa channel activator, NS1619, on rat cerebral artery smooth muscle. *Br J Pharmacol*. 1996;117:119-129.

101. Feng J, Liu Y, Clements RT, et al. Calcium-activated potassium channels contribute to human coronary microvascular dysfunction after cardioplegic arrest. *Circulation*. 2008;118:S46-S51.

102. Gasull X, Ferrer E, Llobet A, et al. Cell membrane stretch modulates the high-conductance Ca2+-activated K+ channel in bovine trabecular meshwork cells. *Invest Ophthalmol Vis Sci*. 2003;44:706-714.

103. Millar JC, Shahidullah M, Wilson WS. Atriopeptin lowers aqueous humor formation and intraocular pressure and elevates ciliary cyclic GMP but lacks uveal vascular effects in the bovine perfused eye. *J Ocul Pharmacol Ther*. 1997;13:1-11.

104. Mittag TW, Tormay A, Ortega M, Severin C. Atrial natriuretic peptide (ANP), guanylate cyclase, and intraocular pressure in the rabbit eye. *Curr Eye Res*. 1987;6:1189-1196.

105. Nathanson JA. Direct application of a guanylate cyclase activator lowers intraocular pressure. *Eur J Pharmacol*. 1988;147:155-156.

106. Diestelhorst M, Krieglstein GK. [The intraocular pressure lowering effect of human atrial peptide]. *Fortschr Ophthalmol*. 1989;86:89-91.

107. Fernandez-Durango R, Moya FJ, Ripodas A, de Juan JA, Fernandez-Cruz A, Bernal R. Type B and type C natriuretic peptide receptors modulate intraocular pressure in the rabbit eye. *Eur J Pharmacol*. 1999;364:107-113.

108. Goldmann DB, Waubke N. [A pilot study on the effect of atrial natriuretic peptide on intraocular pressure in the human]. *Fortschr Ophthalmol*. 1989;86:494-496.

109. Korenfeld MS, Becker B. Atrial natriuretic peptides. Effects on intraocular pressure, cGMP, and aqueous flow. *Invest Ophthalmol Vis Sci*. 1989;30:2385-2392.

110. Wolfensberger TJ, Singer DR, Freegard T, Markandu ND, Buckley MG, MacGregor GA. Evidence for a new role of natriuretic peptides: control of intraocular pressure. *Br J Ophthalmol*. 1994;78:446-448.

111. Yang L, Guan J, Gao S. [An experimental study on effect of atrial natriuretic peptide on intraocular pressure of white rabbits]. *Zhonghua Yan Ke Za Zhi*. 1997;33:149-151.

112. Mittag TW, Tormay A, Ortega M, Severin C. Atrial natriuretic peptide (ANP), guanylate cyclase, and intraocular pressure in the rabbit eye. *Curr Eye Res*. 1987;6:1189-1196.

113. Foerster J, Harteneck C, Malkewitz J, Schultz G, Koesling D. A functional heme-binding site of soluble guanylyl cyclase requires intact N-termini of alpha 1 and beta 1 subunits. *Eur J Biochem*. 1996;240:380-386.

114. Ellis DZ, Dismuke WM, Chokshi BM. Characterization of Soluble Guanylate Cyclase in NO-Induced Increases in Aqueous Humor Outflow Facility and in the Trabecular Meshwork. *Invest Ophthalmol Vis Sci*. 2008.

115. Stasch JP, Schmidt PM, Nedvetsky PI, et al. Targeting the heme-oxidized nitric oxide receptor for selective vasodilatation of diseased blood vessels. *J Clin Invest*. 2006;116:2552-2561.

116. Andersson RM, Aizman O, Aperia A, Brismar H. Modulation of Na+,K+-ATPase activity is of importance for RVD. *Acta Physiol Scand*. 2004;180:329-334.

BIOGRAPHICAL SKETCH

William Michael Dismuke was born in Jacksonville, FL in 1980 to Bill and Nancy Dismuke. He managed to graduate Mandarin High School in 1999 and surprisingly was accepted to attend the University of Florida in the fall of 1999. He graduated in the fall of 2003 with a BS in Botany.